

1 **Grain Size and Beach Face Slope on Paraglacial Beaches of New England, USA**

2

3 **Authors:** Jonathan D. Woodruff¹, Nicholas Venti¹, Stephen Mabee², Alycia DiTroia¹, Douglas

4 Beach¹

5

6 **Affiliations:**

7 ¹Department of Geosciences, University of Massachusetts, Amherst, MA 01003, USA

8 ²Massachusetts Geological Survey, Amherst, MA 01003, USA

9

10 Corresponding author: Jonathan D. Woodruff (woodruff@umass.edu)

11

12 **Keywords:** Beach processes, Glacial sediments, Mixed-sand-and-gravel, Mesotidal, Microtidal,

13 Bimodal

14

15 **Highlights:**

16 • New England is an important region with mixed sand and gravel (MSG) beaches

17 • Grain sizes are controlled primarily by glacial-fluvial and till sediment sources

18 • Beaches have bimodal grain size distributions inherited from paraglacial deposits

19 • Sand characteristics are the primary governor of MSG beach face slopes

20

21

22 **Abstract:**

23 Approximately 100 paired summer and winter transects of beach face slope and intertidal grain
24 size were examined from 18 separate beaches in southern New England that span meso- and
25 micro- tidal regimes. Paraglacial materials provide the principal local sediment source to beaches
26 in this region and grain-size distribution of beaches corresponds to adjacent surficial geology.
27 Stratified glacial fluvial deposits are the primary sediment source to sandier beaches, while till
28 predominantly source the coarser gravel-dominated systems. When aggregated, grain size
29 measurements exhibit a bimodal distribution of medium-to-very-coarse sand (0.25-to-1 mm) and
30 medium-to-very-coarse gravel (10-to-64 mm), with a paucity of grains between 1-10 mm. This
31 bimodality is also common to and likely inherited from the glacial fluvial deposits sourcing the
32 beaches. Beach face slope is observed to increase with median grain size (D_{50}) for finer sandy
33 systems, followed by little-to-no correlation for coarser mixed sand-and-gravel beaches where
34 bulk D_{50} is greater than ~ 1 mm. This finding is consistent with previous trends observed in
35 global beach data sets and highlights the limits of using bulk D_{50} to describe bimodal systems.
36 When gravel is removed from the grain size distribution and the median grain size recomputed
37 for the remaining sand fraction the familiar positive relationship between grain size and slope
38 reemerges. Results support the growing appreciation for sand characteristics as the primary
39 governor of intertidal slope for mixed sand and gravel systems due to its predominant control on
40 beach face permeability and resulting transport processes.

41

42 **1. Introduction**

43 Beaches comprise approximately 31% of the world ice free shoreline (Luijendijk et al., 2018),
44 and serve a multitude of functions including a diverse array of ecological services, key forms of
45 flood defense, and prized locations of recreation and revenue (Martínez et al., 2007). These
46 sedimentary systems are some of the most dynamic landforms on earth and are influenced by a
47 variety of factors that involve waves and tides (e.g. Ivamy and Kench, 2006; Masselink and
48 Short, 1993; Shulmeister and Kirk, 1997), sedimentary supply, sea level change and antecedent
49 conditions (e.g. Billy et al., 2015; Carter et al., 1989; Fitzgerald and Van Heteren, 1999; Forbes
50 et al., 1995a; Kirk, 1980; McLean and Kirk, 1969; Orford et al., 2002), and anthropogenic
51 modifications (e.g. Hein et al., 2019; Horn and Walton, 2007).

52

53 Beach slope and grain size are defining features of beach morphology and the factors that
54 controls these two properties have long been an area of active research. The World War II Waves
55 Project along the Pacific Coast of North America represents an early seminal study on this topic
56 (Bascom, 1951). Five tenets of beach morphodynamics emerged from the project: 1) that the
57 intertidal zones of fine sandy beaches are flatter than those of coarse sandy beaches, 2) that
58 beach material at any place is well sorted, 3) that this sorting occurs by facies, with plunge point
59 (where wave uprush and backwash intersect) being coarsest, followed by the beach berm, the
60 intertidal zone, dune sand, and finally the finest material found with increasing depth off-shore,
61 4) that beaches build seaward and steepen under gently sloping waves and are cut back and
62 flattened by steep waves, and, 5) that wave exposure sorts material into appropriate
63 environments along the coast. The seminal Bascom (1951) paper restricts its scope to sandy
64 beaches, leaving the gravelly beaches for later discussion.

65

66 Subsequent research on coarser beaches indicate that they do not predictably follow the five
67 patterns Bascom (1951) identifies in sandy systems. Regarding the slope/grain size relationship
68 (1), flatter slopes are not always associated with finer grain sizes (McLean and Kirk, 1969) and
69 gravelly beach faces plateau in slope before becoming steeper than sandy beaches as sand
70 becomes excluded from the beach in coarser systems (e.g. Bujan et al., 2019). With respect to
71 sorting (2), on some of these coarser beaches, gravel and sand are well mixed throughout while
72 others follow a composite character with well sorted cobble and gravel in upper facies and well-
73 sorted sand in their intertidal zones (e.g. Bluck, 1967; Jennings and Shulmeister, 2002). Thus,
74 not only are these systems not necessarily well sorted by facies, the facies themselves follow
75 more than one distribution, defying the ranking of faces by sort (3). Regarding wave state and
76 cross-shore morphology described in 4, rather than predictable advance or retreat in response to a
77 dynamic wave regime, sand and gravel beaches instead often undergo various degrees of sorting
78 (Pontee et al., 2004). Finally, with respect to alongshore variability described in 5, instead of
79 materials well sorted into environments along the coast according to wave energy, sediment
80 sources and coastal barriers often bias (and in many cases predominantly control) the type and
81 size of materials appearing on sand and gravel beaches (Fitzgerald and Van Heteren, 1999;
82 McLean and Kirk, 1969).

83

84 Several classification systems for sand and gravel beach systems exist (e.g. Bluck, 1967;
85 Caldwell and Williams, 1985; Carter and Orford, 1993; Jennings and Shulmeister, 2002). Carter
86 and Orford (1993) offer a two-part classification for coarse clastic shorelines consisting of
87 beaches as free-standing or fringing barriers. These are further subdivided into swash or drift-

88 aligned beaches. For Southern New England, USA, FitzGerald and Van Heteren (Fitzgerald and
89 Van Heteren, 1999) define six coastline types based on several parameters including geology,
90 antecedent topography, sediment availability, grain size and wave and tidal energy. This
91 classification system incorporates geomorphology and indirectly includes sediment sourcing as a
92 factor in beach characterization. Jennings and Schulmeister (2002) examine 42 gravel beach sites
93 in New Zealand and develop a three-part classification: 1) pure gravel, 2) mixed sand and gravel
94 (MSG) and 3) composite beaches of steeper upper-intertidal gravel and gently sloping lower-
95 intertidal sands. Horn and Walton (2007) later suggested a 4th beach type where a steeper upper
96 beach is composed of MSG and a lower-tide terrace of sand.

97

98 Predominant regions with detailed studies on MSG systems include the alluvial/fluvial and
99 hinterland sourced beaches of southern New Zealand (e.g. Kirk, 1980; McLean and Kirk, 1969;
100 Shulmeister and Kirk, 1997), as well as the paraglacial shorelines (Forbes and Syvitski, 1994) of
101 the British Isles (Carter et al., 1987; Jennings and Smyth, 1990; Mason and Coates, 2001; Pontee
102 et al., 2004), and eastern Canada (Carter and Orford, 1993; Forbes et al., 1995). The
103 Northeastern coast of United States from the United States/Canadian border south through New
104 York state represents another paraglacial coastline where MSG beaches are prevalent. Studies
105 along this ~13,000 km stretch of coast provide detailed insight on its geomorphic evolution and
106 response to past changes in relative sea level and sediment supply (e.g. Fitzgerald and Van
107 Heteren, 1999; Hein et al., 2014; Kelley, 1987), yet still lacks a regional analyses on grain size
108 and beach slope characteristics. For example, of the 2144 measurements of beach slope and grain
109 size synthesized in a recent global compilation focused to MSG systems (Bujan et al., 2019), no
110 data is available for the Northeastern US.

111

112 This study is focused to grain size and intertidal slope measurements from beaches of
113 Massachusetts, which represents a particularly unique section of the Northeastern US coast in
114 that it: 1) lies at the interface between New England's paraglacial lowlands and Mid-Atlantic
115 Coastal Plain (Fenneman, 1938), 2) spans both micro- and meso- tidal regimes (Redfield, 1980),
116 3) encompasses a wide range of seasonally varying wave conditions (Woolf et al., 2002), and 4)
117 contains a diverse array of geomorphic and grain size characteristics (Fitzgerald and Van
118 Heteren, 1999).

119

120 **2. Regional setting**

121 The study area extends along the entire coast of Massachusetts. Prominent coastal features for
122 this region, from north to south, include the mouth of the Merrimack River, Cape Ann,
123 Massachusetts Bay, Cape Cod and associated islands of Martha's Vineyard and Nantucket, and
124 Buzzards Bay (Fig. 1). During the last glaciation, the region was located near the southern extent
125 of the ice sheet on the uplifted glacial forebulge. The continued relaxation of this forebulge has
126 amounted to ~0.7-1.0 mm/yr of subsidence over the last few millennia (Engelhart and Horton,
127 2012; Peltier, 2004). However, at mean rates of 2.0 mm/yr (Portsmouth, NH) to 3.8 mm/yr
128 (Nantucket, MA) over the past century, sea level rise in the northeastern U.S. (Zervas, 2009)
129 eclipses gentle postglacial isostatic adjustment by nearly 2-to-5 times.

130

131 Cretaceous (and Cenozoic) sediments underlie the glacially derived and postglacial material of
132 Cape Cod and the islands to the south in Massachusetts (Finch, 1823; Oldale and Barlow, 1986;
133 Stone et al., 2018). This area was initially considered part of the New England Physiographic

134 region (Fenneman, 1917, 1916), because here Cretaceous (and Cenozoic) coastal plain sediments
135 lie largely below sea level, whereas this sequence would be extensively exposed further to the
136 south on Long Island in New York State, if it were not covered by post-glacial materials.
137 However, revised geographic interpretation recognizes this area as the northeastern most
138 (exposed) extension of the Atlantic Coastal Plain as it emerges from the continental shelf
139 (DiPietro, 2012; Fenneman, 1938; U.S. National Park Service, 2017). Provenance of sand on the
140 eastern part of Cape Cod supports a significant reworked coastal plain component in material
141 along the coast in this region (Ockay and Hubert, 1996).

142

143 Most of the surficial sediments in New England, including Massachusetts, were deposited during
144 past glaciations in the late Pleistocene (Fig. 1), and largely define the sources of sediment to
145 individual beach systems. Glacial sediments are unevenly distributed over the landscape in New
146 England, resulting in a regional coastline that is generally sediment starved relative to other
147 regions of the U.S. (Fitzgerald and Van Heteren, 1999). However, sediment sources can
148 generally be categorized into three groups (Table 1): 1) stratified deposits - this includes subsets
149 of both, 1a) coarse stratified deposits derived from glacial outwash or kame and river deltas and,
150 1b) fine stratified deposits originating from the erosion of fine-grained glacial marine sediments;
151 2) glacial till; and, 3) mixed sediments consisting of material derived from stratified deposits and
152 glacial till in various proportions.

153

154 Tidal ranges vary depending on location. North of Cape Cod extending to the north shore of
155 Massachusetts the tidal range is roughly 3 m (Table 1). South of Cape Cod the tidal range is
156 approximately 1 m or less (Irish and Signell, 1992; Redfield, 1980). Based on the categorization
157 system of Hayes (1979) study beaches north of Cape Cod are predominantly tide-dominated and

158 beaches south of Cape Cod are classified as wave-dominated (Fitzgerald and Van Heteren,
159 1999). This is with the exception of the more southerly exposed beach at Rockport that is north
160 of Cape Cod but which is a mixed tide-wave energy system (DiTroia, 2019).

161

162 Eighteen beaches were investigated in this study (Fig. 1) and fall into three main geomorphic
163 classes according to the scheme developed by FitzGerald and Van Heteren (1999) for paraglacial
164 barrier beach systems (Table 1; DiTroia, 2019). Salisbury and Plum Island on the north shore of
165 Massachusetts are inlet-segmented (Type 4) beaches composed of long single barrier beaches
166 separated by inlets with significant updrift, river, or offshore glacial fluvial sediment sources.
167 Rockport, Nahant, Revere, Nantasket, Peggotty, Humarock, Marshfield, Barges, East and
168 Horseneck are all headland-separated (Type 2) beaches composed of shorter, narrower barriers
169 separated by bedrock or till headlands providing local, variably sized but less reliable sources of
170 sediment. The remaining beaches, Plymouth, Surf, Low, Miacomet, Town and Sylvia are
171 mainland-segmented (Type 3) beaches comprised dominantly of sand or sand with some gravel
172 derived from glacial outwash and mixed sediment sources (till and outwash), respectively.

173

174 **2.1. Sediment sources for beaches north of Cape Cod**

175 Beginning at the northern extent of the study area, Salisbury and Plum Island beaches represent
176 two systems sourced predominantly from relic fluvial deltaic deposits. The Boston area and
177 north shore of Massachusetts underwent a marine incursion during initial ice retreat followed
178 closely by isostatic rebound that produced a rapid relative sea level drop allowing the post-
179 glacial Merrimack River to deposit a veneer of fluvial sediments and an offshore delta (Fig. 1),
180 (Barnhardt et al., 2010; Oldale et al., 1993; Stone et al., 2006). Delta foreset beds overlying
181 marine silts and clays are evident in offshore seismic records (Barnhardt et al., 2009). Holocene

182 marine transgression reworked the delta and fluvial deposits providing the primary source for
183 sediments along with riverine contributions from the adjacent Merrimack River.

184

185 The Rockport site, known locally as Long Beach, is located just south of Salisbury and Plum
186 Island on the rocky peninsula of Cape Ann. Of all the sites, the sediment source for Rockport is
187 one of the most difficult to assess. The beach is located in an area of numerous granite bedrock
188 outcrops interspersed with pockets of very thin glacial till (<1-2 m) (Stone et al., 2006). The
189 Rockport site is enclosed on each end by two bedrock headlands and comprised mostly of
190 medium sand at low and mid tide but underlying cobbles and gravel are exposed at high tide in
191 the winter. There is a marsh/swamp located behind the beach. During Holocene marine
192 transgression it is likely marsh/swamp deposits were much farther seaward and the beach
193 transgressed over the deposits as it migrated shoreward during sea level rise (Emery et al., 1967).

194

195 The Nahant site and Revere Beach are both sourced by fine-grained stratified deposits (Table 1)
196 that underlie later post-glacial deposits throughout the Boston area (Fig. 1) (Stone et al., 2018).
197 These fine-grained deposits are marine silts and clays deposited prior to ice retreat when relative
198 sea level was 31 to 33 m higher than modern sea level (Stone et al., 2004b). It should be noted
199 that Revere underwent major restoration in the 1990s and is nourished annually with up to 10
200 tons of fine sand to support a sandcastle building contest during the summer. Nahant also
201 underwent a dune restoration project in 2014.

202

203 Nantasket Beach, located immediately south of Boston is adjacent to several till-based drumlins,
204 including some eroded offshore, that served as the main source of sediment to the beach (Fig. 1).

205 However, it was common practice to remove the gravel armor that appeared after each winter,
206 resulting in a lowering of the beach profile over time (FitzGerald and Rosen, 1988). This may
207 have skewed its grain size to become somewhat finer than would otherwise be expected from a
208 glacial till source. It is estimated that 96,000 m³ of cobbles and gravel were removed from the
209 beach between 1950 and 1968 by beach maintenance crews (USACE, 2012).

210

211 Along the south shore of Massachusetts Bay, Peggotty, Humarock and Marshfield beaches are
212 mixed beaches receiving sediment from the erosion of both coarse stratified deposits (glacial
213 outwash) and glacial till (Table 1; Fig. 1) (Stone et al., 2018). The Plymouth site is located to the
214 south of Marshfield and lies adjacent to an extensive, glacial outwash deposit characterized by
215 very hummocky, kame and kettle terrain (Fig. 1) (Stone et al., 2012).

216

217 **2.2. Sediment sources for beaches south of Cape Cod**

218

219 Miacomet and Low Beaches are located on the island of Nantucket. Similar to Plymouth,
220 Miacomet and Low are also sourced from glacial outwash (Fig. 1), but are located approximately
221 4 km from the late Wisconsinan terminal moraine whereas the glacial outwash deposits near
222 Plymouth represent a more distal and finer facies of the outwash morphosequence (Koteff and
223 Pessl, 1981; Stone et al., 2004a).

224

225 Surf Beach, located on the south side of Cape Cod (Fig. 1), is situated just east of the contact
226 between the Buzzards Bay recessional moraine and the “Crooked Pond deposits”. The Crooked
227 Pond deposits are near-ice-marginal glaciofluvial fan deposits onlapping the Buzzards Bay
228 moraine and eventually overlying the distal end of pitted outwash plains to the east (Stone and

229 Stone, 2019). These deposits contain cobbles and gravel and were noted as the “very coarse-
230 grained Mashpee pitted plain deposits” recognized by Mather et al. (1942) and Masterson et al.
231 (1997) but not previously mapped (Stone and Stone, 2019).

232

233 Town and Sylvia Beaches are located on the island of Martha’s Vineyard (Fig. 1) and are
234 comprised of sediment from a mixture of two surficial deposits, till associated with the late-
235 Wisconsin terminal moraine and glacial outwash. The terminal moraine deposits are comprised
236 mostly of boulders and sandy till (Stone and DiGiacomo-Cohen, 2006). Town Beach is sourced
237 primarily from sandy till but there is a veneer of outwash overlying the till deposits (Oldale and
238 Barlow, 1986). At Sylvia Beach, the terminal moraine is buried by thicker deposits of outwash.
239 Accordingly, Sylvia Beach is sourced by a higher proportion of outwash than Town Beach,
240 which contains a higher gravel/cobble component.

241

242 To the west of Martha’s Vineyard lies the Elizabeth Island chain, formed from the Buzzards Bay
243 recessional moraine. Barges Beach is located on Cuttyhunk, the southwesternmost island of the
244 Elizabeth Islands, and is composed mostly of gravel and cobbles derived by the erosion of the
245 recessional moraine (Fig. 1). Finally, Horseneck and East Beaches lie to the west of Buzzards
246 Bay, along the westernmost portion of mainland Massachusetts bordering the State of Rhode
247 Island, and are sourced by the direct erosion of glacial till in widely distributed ground moraines
248 (Fig. 1).

249

250 **3. Materials and methods**

251 Beaches in this study were selected in collaboration with the Massachusetts Office of Coastal
252 Zone Management in order to characterize the grain size distribution and beach slope in the

253 intertidal zone. Between 2 and 10 intertidal transects were conducted for each of the sites
254 depending on the length of the beach and accessibility. Transect positions were chosen at
255 representative locations along the beach and equally spaced when possible. At each transect at
256 least three separate samples were collected at near 1) high-tide, 2) mid-tide and 3) low-tide.
257 When possible, additional samples were collected along storm berms and dunes but for brevity
258 are not presented here. To assess seasonal variations in grain size distribution and slope, all
259 transects along beaches were sampled and surveyed twice, once at the end of the summer and
260 then revisited again at the end of the winter season. Surface sediments from the top 15-30 cm
261 were collected from sites primarily composed of sand and pebbles (i.e. < 64 mm), and brought
262 back to the University of Massachusetts in Amherst, MA for analysis. Exclusively sand samples
263 were collected in 1-liter (1-quart) bags, predominantly sand samples were collected in 4-liter (1-
264 gallon) bags and mixed sand and pebble samples in 19 -liter (5 gallon) buckets. Areas comprised
265 primarily of cobbles and boulder (> 64 mm) were measured in the field using a gravelometer and
266 standard pebble count techniques (Wolman, 1954).

267

268 Sediment samples were washed and dried thoroughly to remove salt and debris (sticks, seaweed,
269 etc.). Each sample was weighed and sub-divided into fractions greater and less than 4 mm.

270 Distributions for grains greater than 4 mm were obtained via standard sieving techniques
271 (Udden, 1914; Wentworth, 1922)(Udden, 1914; Wentworth, 1922). Grain size distributions for
272 sample fractions < 4 mm were measured on a CAMSIZER digital particle size analyzer capable
273 of measuring particles between 30 μm and 4 mm (Switzer and Pile, 2015). A total of 907 grain
274 size analyses and 86 pebble counts were conducted (See Section 7 for data availability).

275

276 Inter-tidal beach slope for each transect was obtained using a using a Real Time Kinematic
277 (RTK) GPS survey system or a total station survey system tied to local benchmarks. Markers
278 were placed at the head of each transect so the transects could be reoccupied the following
279 season. A total of 235 transects were completed.

280

281 Off-shore wave conditions were independently reconstructed for each beach based on publicly
282 available results from the United States Geological Survey (USGS) Coupled Ocean-
283 Atmospheric-Wave-Sediment Transport (COAWST) model (Warner and others, 2010), and
284 using the nearest deep-water grid cell to each respective beach. Modeled average wave heights
285 directly off-shore of the sites in the 30-days preceding seasonal surveys ranged between 0.4 m
286 and 2.5 m (bars in Fig. 2A), with storm-induced 12-hr -averaged maxima over the same intervals
287 between 0.9 m and 7.6 m (circles in Fig. 2A). North of Cape Cod modeled wave heights were
288 largest overall for Rockport Beach, which is south facing and located on the prominent rocky
289 exposed headland of Cape Ann (Fig. 1). South of Cape Cod the southern facing beaches of Low
290 and Miacomet on Nantucket were the largest. Smallest wave heights south of Cape Cod were
291 modeled for the nearby beaches of Sylvia and Town, located on the northeast coast of Martha's
292 Vineyard facing back to the Cape Cod mainland.

293

294 In terms of seasonality, modeled winter wave heights were consistently higher than summer at
295 all sites (Fig. 2A), with the more exposed shorelines experiencing the greatest increases overall
296 (e.g., an increase in 12-hr-averaged max wave heights between summer and winter of > 5 m at
297 Rockport and 2-to-3 m for Low and Miacomet). In contrast, minimal seasonal differences in

298 wave height occurred at more sheltered sites including the northeast facing Martha's Vineyard
299 beaches of Sylvia and Town, where winter increases did not exceed a few cm.

300

301 **4. Results**

302 **4.1 Regional and seasonal changes in grain size and beach face slope**

303 For summer surveys a regional median grain size of 0.8 mm was observed south of Cape Cod
304 and 0.4 mm for the north (Fig 2B). These regional medians increased in the winter surveys to 1.2
305 mm for the south and 0.6 mm for the north. Grain sizes were therefore greater where wave
306 heights were higher south of Cape Cod and during the season of greater wave activity. However,
307 these regional differences were less than the overall variance observed in grain size distributions
308 from site to site, which ranged by an order of magnitude, and reveal the diverse types of sandy to
309 MSG beaches evident in both tidal regions. Seasonally, grain size distributions coarsened most
310 significantly in the winter for MSG systems (e.g. Pegotty, Humarock, Town, Surf, Barges, East
311 and Horseneck), due in part to an apparent winnowing of sands from these locations. Sandier
312 systems also tended to coarsen in the winter, although less significantly than at MSG locations,
313 and with the exception of Nahant and Plymouth, where a slight winter fining was observed.

314

315 Active beach slopes of mesotidal beaches north of Cape Cod were predominantly flatter than
316 microtidal sites to the south (Fig. 2C; slope medians of ~ 0.06 and ~ 0.12 for meso- and macro-
317 tidal regions, respectively). This finding is consistent with past observations of beach widths
318 generally increasing with increasing tidal range (e.g. Masselink and Short, 1993). However,
319 similar to grain size, intertidal slopes for individual beaches varied greatly relative to these
320 regional medians, and did not necessarily correlate with bulk grain size. For example, beach face

321 slopes at the meso-tidal and predominantly sandy Plum Island site were similar or steeper than a
322 majority of slopes for coarser MSG systems at microtidal locations (e.g. Town, Surf, Barges and
323 Horseneck). The steepest beaches observed in the study were during summer at the
324 predominantly sandy Low Beach and during winter at the MSG East Beach. Although
325 predominantly sandy, the steeper Plum Island and Low Beaches did exhibit some of the coarsest
326 sand fractions of meso- and micro- tidal regions (Fig. 2B), while the lack of a gravel mode
327 resulted in significantly lower median bulk grain sizes when compared to MSG sites. The
328 shallowest beach face slopes in the study were observed at Nahant (Fig. 2C), which also was the
329 finest of all beaches sampled (Fig. 2B). At individual sites most beach face slope distributions
330 remained relatively similar seasonally, although regional medians revealed a slight drop in slope
331 during winter at mesotidal locations and a slight winter steepening at microtidal sites (Fig. 2C).
332 The most significant winter steepening was observed at the MSG beaches of Humarock, East and
333 Horseneck and finer grained Miacomet, while the most significant decreases in winter slopes
334 were at the finer grained beaches of Rockport and Low.

335

336 **4.3 Grain size relative to surficial geology**

337 Observed winter coarsening in regional medians of grain sizes indicate some oceanographic
338 control on beach characteristics (e.g. dashed orange and blue lines in Fig. 2A and 2B). However,
339 some of the finest-grained sandy beaches exhibited the greatest off-shore wave height, including
340 Low and Miacomet on Nantucket, while more sheltered nearby beaches of Sylvia and Town on
341 Martha's Vineyard were substantially coarser (Fig. 2A and 2B). Such inconsistencies indicate
342 that oceanographic effects are not the predominant control on grain size at the sites, supporting a

343 basis for previous coastal classifications for this region that consider underlying geologic
344 conditions.

345

346 Grain sizes observed on the beaches in this study generally correspond to the relative grain sizes
347 observed within their respective source material (Fig. 3). For example, beaches associated with
348 fine stratified deposits were the finest grained, followed by coarse stratified deposits, and then
349 those sourced by a mixture of stratified deposits and till. Beaches sourced purely by till exhibited
350 the greatest range of grain sizes. Rockport and Nantasket appear to be anomalous. Though till
351 was available locally to these beaches, they are finer than expected when compared to other till-
352 sourced beaches in the study. With respect to sorting, grain size distributions obtained from
353 beaches either partially or fully sourced by till were poorly to very-poorly sorted (also with the
354 exception of Rockport). In contrast, a majority of beaches sourced by stratified drift are
355 moderately-to-well sorted (with the exception of Revere).

356

357 There is a marked distinction in grain size characteristics between beaches purely sourced by
358 stratified drift relative to ones sourced in part or fully by coarser and more poorly sorted till. As
359 noted, Rockport and Nantasket are presumably till-sourced but are anomalously fine-grained
360 beaches. We suspect the reworking of barrier/marsh material during transgression at Rockport
361 and the routine removal of gravel from Nantasket are responsible for them being anomalously
362 fine. Peggotty Beach is also somewhat finer grained relative to other mixed-source beaches in
363 the study. Due to public access restrictions, transects from Peggotty were limited to the finer
364 northern section of the beach, where overwash material is returned in spring following winter
365 storms. This sampling bias could therefore provide at least a partial explanation for the

366 somewhat finer grains observed at the site and the lack of a predominant gravel mode evident
367 upon visual inspection to the south. Minus these discussed exceptions, however, sediment source
368 appears to exhibit a predominant control on grain size characteristics for beaches within the
369 study. In contrast, grain-size distinctions based on oceanographic conditions, when separated into
370 meso- and micro-tidal regions, or seasonal shifts in grain size due to summer-winter changes in
371 wave climatology are more subtle (Fig. 2).

372

373 Most grain size distributions for partially or fully till sourced beaches exhibit a bimodal
374 distribution of sand and gravel. The gravel mode for these systems result in overall coarser
375 sediments when using common metrics such as the median or bounds of the middle quantiles
376 (e.g. box plots in Fig. 3). However, when focused purely to the sand fraction, till sources systems
377 were generally finer than the unimodal pure-sand beaches sourced by coarse stratified deposits
378 (Fig. 3). Fine stratified deposits exhibited the finest sand fractions, followed by pure till sourced
379 systems, then those sourced by a mixture of till and stratified deposits, and finally systems
380 sourced purely from coarse stratified deposits.

381

382 Where gravel appears on the beach, we generally find it distributed throughout the exposed
383 cross-shore facies, consistent with the “mixed” class of sand and gravel beach of Jennings and
384 Schulmeister (2002). Synthesis of the bulk grain-size distribution of intertidal mixed sand and
385 gravel (at least 5% > 2 mm) samples are presented in Fig. 4 (n=454) and exhibit a distinct
386 bimodal distribution. This bimodality spans the entire study region and shows two separate peaks
387 between medium-to-very-coarse sand (0.25 mm to 1 mm) and medium-to-very-coarse gravel (10
388 mm to 64 mm). These peaks are separated by a local minimum centered at approximately 1 to

389 10 mm. However, the overall median of the distribution occurs at 2 mm (sand/gravel transition),
390 resulting from the coalescence of the separate sand and gravel modes. Independent analyses of
391 just bucket and bag samples (n=368), which were mechanically sieved also show similar
392 bimodality. Sand and gravel modes present in Fig. 4, as well as the paucity of grains between 1-
393 10 mm, are therefore likely not an artifact of combining distributions from sieving and pebble
394 counts, but rather a persistent feature of sand and gravel beaches of southern New England.

395

396 **4.4. Beach face slope versus median grain size**

397 In Fig. 5 data is separated further into low, mid and high tide samples to assess intertidal trends
398 and generalizable consistencies. Comparison of median grain size and beach face slope data from
399 this study is generally consistent with the global data set compiled by Bujan et al. (2019).

400 Primary correspondence at all inter-tidal locations when compared to the broader Bujan et al.

401 (2019) global composite include: 1) an increase in beach face slope with grain size for D_{50} values

402 below 1 mm, 2) an upper limit in beach face slope of roughly 0.2, and 3) poor correlation

403 between grain size and slope for D_{50} values that exceed ~ 1 mm. In general, our data also exhibit

404 a plateau in slope beyond 1 mm that occurs within an approximate range of 0.1 and 0.2.

405 However, a number of slope observations beyond a D_{50} of 1 mm exist well below this range in

406 slope, particularly at mid- and high- tide locations. Categorizing grain size measurements by

407 their degree of sorting reveals that samples with D_{50} values between 1-10 mm are all poorly

408 sorted, likely reflecting varying contribution of grains within abutting sandy and gravel modes

409 shown in Fig. 4. In contrast, moderately-to-well sorted samples all exhibit median grain sizes

410 that overlap well with the previously discussed sand (0.25 mm to 1 mm) or gravel (16 mm to 64

411 mm) modes, and with a skew towards better sorting at high-tide locations.

412

413 Testing a common power-law fit to bulk D_{50} vs. beach face slope data results in a significant
414 under-prediction of slope when compared to previous data available from pure gravel beaches
415 (Fig. 6A). However, an improved fit with pure gravel systems was obtained when recomputing
416 the median grain size on just the sand component from our mixed sand and gravel beaches (*i.e.*,
417 removing the gravel component in the calculation, red plus signs in Fig. 6B).

418 **5. Discussion**

419 **5.1. Origins of beach bimodality**

420 Bimodality in grain-size distributions on southern New England beaches (Fig. 4), indicates two
421 separate and distinct sand and gravel populations which likely have very different and divergent
422 behaviors. Observed winter coarsening, particularly for MSG systems (Fig. 2), is primarily due
423 to the winnowing of sand during greater wave activity that is later returned during the summer
424 months. Anecdotal evidence for this phenomenon was observed first hand in the field with the
425 rapid erosion of sands by storms followed by rapid deposition during surveys at the beaches of
426 Barges, East and Humarock. In contrast, the separate gravel mode in Fig. 4 persists throughout
427 our seasonal surveys (Fig. 2B), and is restricted to locations nearest to its till-derived source (Fig.
428 3). This is particularly true for headland separated beaches where gravel exchange between
429 systems is unlikely (Fig. 1). Thus, our observations support gravel behaving more as a passive
430 lag deposit while sand represents the more active participant (e.g. Bluck, 1967), and as such,
431 exhibits the greater control on active beach slope (Fig. 6). However, beach bimodality is difficult
432 to explain solely by in situ processes since this high energy environment is continually reworked
433 by waves, which in turn provides a mechanism for sorting (Inman, 1949). A poorly sorted
434 bimodal sand and gravel beach therefore implies a sedimentary environment in disequilibrium,

435 as is common for most environments where sediments are derived from post-glacial deposits
436 (e.g. Easterbrook, 1982).

437

438 Close relationships between glacial and post-glacial deposits and beach grain size described here
439 would suggest allochthonous sourcing of beach material, consistent with many models for sand
440 and gravel beaches generally. In Alaska (Hayes and Ruby, 1994), the British Isles (Carter and
441 Orford, 1984), Atlantic Canada (Orford et al., 2001), and New England (Fitzgerald and Van
442 Heteren, 1999), glacial till and post-glacial coarse stratified deposits intersect the coast.

443 Similarly, coastal reworking of adjacent ancient coarse-grained deposits mix with sand in
444 Taiwan (Hsieh et al., 2004), the northern Mediterranean (Ortega-Sánchez et al., 2017), and Baja
445 California (Emery, 1955). Alternatively, fluvial inputs combined with rapidly eroding
446 hinterlands, as in New Zealand (Bluck, 1967; Kirk, 1980) and the U.S. Pacific Coast (Bascom,
447 1951) can deliver both coarse and fine grained sediments directly to the beach.

448

449 McLean and Kirk (1969) provides one of the first accounts of beach bimodality based on surveys
450 along the northeast shoreline of the South Island of New Zealand. Building on Folk and Ward
451 (1957), sediment source was determined as the primary control on bimodal beach characteristics.
452 Oceanographic processes (e.g. waves and tides) were evaluated as secondary controls manifested
453 as variance around primary grain size trends. Later measurements by McLean (1970), however,
454 revealed unimodal sediments at size fractions between bimodal gravel and sand peaks. The in-
455 situ breakdown of parent greywacke rock derived from steep neighboring terrane was
456 hypothesized for grain sizes in all size fractions and it was concluded that sediment source might
457 not always be dominant in controlling beach grain size characteristics. Bimodal grain-size

458 distributions have more recently been noted at other locations where MSG beaches are prevalent,
459 but with differences in the size of predominant modes and no unifying resultant grain size gap
460 (e.g. Bergillos et al., 2016; Horn and Walton, 2007; Pontee et al., 2004).

461

462 Bimodality in glacial deposits is well established (e.g. Easterbrook, 1982), where fine and coarse
463 grained modes in basal tills results from a combination of crushing (clast size) and abrasion
464 (matrix mode), (Dreimanis and Vagners, 1971). Transport breaks the rock down into two
465 components – one is clast size consisting of rock fragments, the second is till matrix consisting
466 of mineral fragments. Near the glacier source the clast size mode is always larger than matrix
467 mode but with increasing transport distance the matrix mode grows larger relative to the clast
468 mode (Dreimanis and Vagners, 1971). The gap between clast mode and matrix mode is thought
469 to be the dividing line between pure crushing by glacier movement and abrasion with the
470 threshold at 2 mm (Haldorsen, 2008). Bimodal distributions have been observed also in glacial
471 till lag deposits located offshore of the New England Coast (Pratt and Schlee, 1969).

472

473 Bimodality is also a characteristic of river deposits (e.g. Maizels, 1993; Rădoane et al., 2008;
474 Sambrook-Smith, 1996; Sambrook-Smith and Feruson, 1995) and by extension glacio-fluvial
475 systems. In narrower valleys bimodal distributions can be caused by overlapping two grain size
476 distributions of different origins. The coarse material is sourced by abrasion and hydraulic
477 sorting whereas the source of sand material may reach the river bed through hillslope erosion.
478 Rădoane et al. (2008) report two distinct peaks in Romania with minima in grain size between 1
479 and 8 mm. In other instances, high flows move coarse material while lower flows bring in sand
480 which fills the interstices (Eynon and Walker, 1974). Mean velocities in excess of 300 cm/sec

481 will move the gravel as bed load while sand is transported in suspension. After the gravel is
482 deposited under lower flow conditions, the sand filters in creating strongly bimodal distributions
483 (Eynon and Walker, 1974).

484

485 Bimodality in rivers are also commonly discussed in the form of abrupt gravel to sand transitions
486 (e.g. Ferguson et al., 1996; Parker and Cui, 1998; Sambrook-Smith and Ferguson, 1995; Shaw and
487 Kellerhals, 1982). These gravel to sand transitions (GST) often migrate over time (Ferguson,
488 2003; Marr et al., 2000; Robinson and Slingerland, 1998), resulting in a depositional sequence
489 that is as a whole distinctly bimodal (Marr et al., 2000; Paola et al., 1992). No universal theory
490 currently exists to explain GST (Dingle et al., 2020), although the phenomena is well
491 documented as well as a resultant 1-10 mm gap in grain size similar to that observed in Fig. 4
492 (e.g. Dade and Friend, 1998; Wolcott, 1988). Possible explanations for this grain size gap
493 include grain-size dependent changes in particle breakdown or comminution (Jerolmack and
494 Brzinski, 2010), nonlinearities in bedload transport (Ferguson, 2003), transitions from viscous-
495 to-turbulent dependent sediment suspension thresholds (Lamb and Venditti, 2016), a switch from
496 washload to suspended/bedload transport of sands (Dingle et al., 2020), and shifts from gravel
497 beds to cohesive channel banks as the predominant control on channel geometries for gravel and
498 sandy channels (Dunne and Jerolmack, 2018).

499

500 Current theory predominantly prescribes fluvial bimodality to along channel changes in river
501 transport and is less relevant to wave-induced transport in beach settings. This is with the
502 exception potentially of the ablation mechanisms put forth by Jerolmack and Brzinski (2010).
503 However, unimodal beaches with distributions between 1-10 mm have been observed previously

504 (e.g. McLean, 1970) and suggest that the bimodality observed in our New England beach
505 systems are not globally generalizable, but rather a characteristic common to systems sourced
506 predominantly from glacial and fluvial deposits where the presence of a 1-10 mm grain size gap
507 is well established. Thus, we interpret the bimodality in our paraglacial beach systems to be
508 largely inherited from the glacial and fluvial deposits upon which they are derived, yet with
509 resulting behaviors including grain size vs. slope relationship that are unique (e.g. Fig. 6),
510 relative to the unimodal sandy systems described in detail by Bascom et al. (1951).

511

512 **5.2 Processes governing beach face slope on mixed bimodal beaches**

513 Many have noted previously the likely impacts of bimodality on relating grain size to beach face
514 slope (e.g. Zenkovich, 1967), first with respect to the ineffectiveness of a single metric such as
515 median or mean grain size in describing bimodal grain size distributions (Sambrook-Smith et al.,
516 1997), and second for the predominant roll of the sand fraction in determining beach
517 permeability and in turn sediment transport and morphology (e.g Holmes et al., 1996; Mason et
518 al., 1997; Mason and Coates, 2001; Quick and Dyksterhuis, 1994).

519

520 Bascom (1951) invites the use of median grain size (D_{50}) to describe beach facies because
521 excellent sorting generally allows this single metric to adequately capture these environments.
522 However, where sediment is not well sorted, and particularly for bimodal beaches, there is no
523 reason to expect median or mean grain size to correspond to beach face slope. Many of the
524 beaches described here include gravel (and cobble), yet follow the slope predicted by their sand
525 components (Fig. 6B), while bulk median grain size cannot predict slope for these coarser
526 bimodal systems (Fig. 6A).

527

528 All the beaches in the Massachusetts study include a substantial sand component (>25% for bulk
529 seasonal distributions, Fig 2B), and given sand's leading role in both transport and permeability,
530 it appears likely that the characteristic of this sand component provides a predominant control on
531 beach slope (Fig. 6B). As at other sand and gravel beaches (Jennings and Shulmeister, 2002),
532 there appears to be a high threshold (Masselink and Li, 2001) for coarse material content before
533 beach face slope again begins to correspond to the bulk median grain size (Bujan et al., 2019).

534

535 Our work highlights the need for additional research on the predominant processes and potential
536 governors of beach face slope for bimodal beaches common to the glaciated New England
537 region. Past works provide support for two key aspects of sand preferentially controlling beach
538 morphology in bimodal systems. First, fine grains are transported more easily, can be suspended
539 more easily, and fall more slowly, thus potentially playing a more dynamic role in determining
540 the morphology of bimodal mixed sand and gravel systems. Second, and likely more
541 importantly, finer sands restrict the hydraulic conductivity of the beach, and, in turn, the degree
542 of swash infiltration and effluent during rising and falling tides, respectively. Hydraulic
543 conductivity increases with grain size diameter in a non-linear fashion: slowly in sand, then
544 increasingly rapidly in gravel (Buscombe and Masselink, 2006; Horn, 2002; Krumbein and
545 Monk, 1943). On timescales of tidal fluctuations, high porosity of gravel ($D_{50} > 3\text{mm}$) allows
546 good circulation; intermediate porosity of coarse sand ($3\text{ mm} > D_{50} > 0.5\text{ mm}$) allows poor
547 circulation; low porosity of medium and fine sand ($D_{50} < 0.5\text{ mm}$) allows virtually none
548 (Bagnold, 1940). The amplitude and phasing of water table fluctuations at the beach face with
549 respect to the tide are determined by the porosity, and thus the grain size of beach material

550 should determine whether infiltration into and effusion from material shape the beach face
551 (Masselink and Li, 2001).

552 As mentioned, finer sands not only restrict groundwater flow, but smaller grains are carried more
553 easily due to their lower fall velocities, and the slope of the beach face moderates the speed of
554 the uprush and backwash, further sorting sand. The uprush moves sand landward more
555 effectively than the backwash because of its faster speed, shorter duration, and enhanced
556 suspension of sediments in the boring action of breaking waves (Masselink and Hughes, 1998).
557 Swash infiltration becomes an increasingly trivial process for medium and fine sand (<0.5 mm)
558 (Bagnold, 1940), so fall velocity becomes the dominant factor controlling slope for finer sand
559 beach faces (Dubois, 1972). Too coarse and the sand becomes stranded on the berm in the
560 uprush; too fine and the sand is carried deeper offshore (Bascom, 1951). Thus, waves and tides
561 sort sand effectively in the intertidal zone, with slope corresponding to the appropriate grain size
562 (Bascom, 1951).

563 Following this explanation for beach slope, the plateau in slope near the sand-gravel transition
564 noted by Bujan et al. (2019) could in part be caused by mixed sand and gravel systems where
565 reduced slopes are limited by their sand component. Comparison to the mixed sand and gravel
566 versus pure gravel beaches of Jennings and Schulmeister (2002) included in the Bujan et al.
567 (2019) metanalysis illustrates this aspect of the aggregate data set. Specifically, the lower
568 porosities and fall velocities of the substantial sand components on these beaches shape the
569 shoreface resulting in shallower slopes, as observed in many of the Massachusetts beaches
570 studied here. Considering coarser beaches generally, however, with increasing median grain size
571 (cobble), we suspect that a diminishing sand component becomes increasingly excluded from
572 these higher energy systems, explaining why slopes of cobbly beach faces composed

573 predominantly of pure-gravel more reliably steepen beyond mixed sand and gravel systems with
574 median grain size in the gravel range (e.g. Fig. 6B; Jennings and Schulmeister, 2002).

575

576 **5.3 Oceanographic Impacts**

577 Oceanographic factors may provide additional secondary explanations for the scatter observed
578 between grain size and slope along the Massachusetts beaches, particularly when gravel is
579 removed and comparisons are made between median sand size and beach face slope. Increasing
580 tidal range typically corresponds to an increase in beach width (Masselink and Short, 1993), and
581 could in part explain the shallower slopes for the meso-tidal beaches relative to their micro-tidal
582 counterparts (Fig. 2C). However, the same general sand D_{50} vs. slope relationships hold even
583 when observations are categorized into their predominant oceanographic setting (Fig. 7). This is
584 true both in terms of micro- vs. meso-tidal ranges (Fig. 7, top right panel) and summer-winter
585 wave climatology (Fig. 7, bottom right). If true, the general decrease in bulk grain size observed
586 for our meso-tidal relative to micro-tidal systems would provide support for feedbacks, where
587 beach slope is adjusted in part via a reduction in grain size for these systems.

588

589 We suspect tidal regime to be the predominant control on regional differences in slope north and
590 south of Cape Cod. However, an alternative explanation for greater slopes for beaches south of
591 Cape Cod is that there is a paucity of finer-grained beaches in this region as a result of its unique
592 depositional setting. Whereas in the north fine-grained glaciomarine deposits are widespread
593 across Massachusetts Bay and Cape Cod Bay, many of the beaches south of Cape Cod are
594 proximal to the late Wisconsinan terminal moraine or the Buzzards Bay recessional moraine.
595 Accordingly, this close proximity to the ice margin may have resulted in higher depositional

596 energy producing a general coarsening of sand within associated stratified deposits. The southern
597 mixed till/stratified source beaches of Sylvia, Town and Surf show some evidence of courser
598 sands when compared to the northern beaches of Peggotty, Humarock and Marshfield (Fig. 3).
599 However north-south differences for other sediment sourcing categories in Fig. 3 are less
600 conclusive.

601

602 With respect to oceanographic conditions, waves provide another potential control on beach
603 characteristics in addition to tides (e.g. Masselink and Short, 1993). Primary evidence for waves
604 controlling grain size at our sites include a general coarsening in median grain size for the winter
605 surveys relative to summer (blue vs. orange dashed lines in Fig. 2B). When categorized by
606 season, winter beach face slopes appears to plot slightly lower than its summer counterpart at the
607 northern meso-tidal locations (Fig. 2C), consistent with flattening of the beach during landward
608 translation of the face during winter. Although we observed clear landward retreat of some of the
609 sandier beaches (Salisbury, Peggotty, Rockport, Low) during winter, on coarser beaches
610 advance/retreat results are mixed from one transect to the next and the beach appeared to move
611 little in aggregate seasonally. We therefore interpret the general summer-to-winter bulk
612 coarsening in Fig. 2 as representing a partial removal of some of the sand fraction in the surface
613 layer of these beaches. An increase in winter wave activity therefore appears sufficient enough to
614 winnow sands and coarsen the resultant median grain size (Fig. 2B), but the amounts removed
615 are insufficient to cause a significant, generalizable seasonal change in beach face slope (Fig.
616 2C).

617

618

619 **5.4 Future Work**

620 Considering sand versus MSG beaches, we return to Bascom's five tenets with greater
621 appreciation for how coarse material interrupts patterns predicted for otherwise sandy systems.
622 Regarding 1) that the intertidal zones of fine sandy beaches are flatter than those of coarse sandy
623 beaches, we find that this holds true for the sand fraction. Future work might build on how sand
624 continues to control beach slope when gravel is included. Regarding 2) that beach material at any
625 place is well sorted, we find this true for the sand fraction, though not true for bulk material.
626 Previous studies recognize both mixed (*e.g.* this study) and composite classes of sand and gravel
627 beaches, where good sorting at any point is followed. Why one form or the other appears along
628 the coast is an open question in beach research. To 3) that sorting occurs by facies, with plunge
629 point (where wave uprush and backwash intersect) being coarsest, then summer berm, the
630 intertidal zone, dune sand, and the finest material with increasing depth under water, we find a
631 slightly different pattern with the coarsest material found stranded within high-tide facies.
632 Instead of clear evidence for 4) that beaches build seaward and steepen under gently sloping
633 waves and are cut back and flattened by steep waves, we find that high-energy waves winnow
634 sand to leave a coarser winter beach face, whereas sand becomes reincorporated under low
635 energy summer waves. MSG beaches use a step to accommodate wave energy (*e.g.* Masselink et
636 al., 2010), which may explain insensitivity in beach face slope and facies positions to changing
637 wave climate observed here. Finally, we cannot resolve 5) that wave exposure sorts material into
638 appropriate environments along the coast. Along the complex postglacial coast the general
639 distribution of the sand component's distribution on the beach is poorly understood. Further
640 research is needed to evaluate how availability of nearby sand deposits determines fine beach

641 material versus in situ sorting of this sand fraction into appropriate coastal environments by
642 oceanographic processes.

643

644 **6. Conclusions**

645 Post-glaciated beaches in the New England region are relatively unique to the U.S., yet represent
646 important examples of the global subset of beaches composed of both sand and gravel. Glacial
647 till and outwash/fluvial deposits are the primary sources of gravel and sand to local beaches in
648 the region, respectively, and the relative contribution of these two sources serve as the
649 predominant control on aggregate beach grain size. Oceanographic factors exhibit secondary
650 controls with an increase in beach slope for micro- versus meso-tidal systems, and a general
651 summer-to-winter coarsening due to the seasonal winnowing of sands. Combining all beach
652 grain size distributions from the region reveals two separate modes of medium-to-very-coarse
653 sand and medium-to-very-coarse gravel separated by a lack of grains between 1 and 10 mm. This
654 gap in grain size is common to paraglacial and fluvial deposits upon which sediment to regional
655 beaches in New England are derived and suggests an allochthonous rather than autochthonous
656 cause. Median grain size or D_{50} is a common metric used for predicting active beach slope for
657 unimodal beaches, but our work supports past observations on D_{50} being less effective when
658 applied to bimodal mixed sand and gravel beaches. Similar to these past studies we observe
659 beach slope predictably increases with grain size up to a bulk D_{50} of ~ 1 mm, and a lack of
660 correspondence beyond this median size. For coarser mixed sand and gravel systems the D_{50} of
661 the sand fraction better predicts beach face slope, and follows a similar D_{50} vs. slope relationship
662 as that observed using bulk D_{50} for finer, sandy unimodal beaches. Comparisons to pure gravel
663 beaches reveals that a relatively high fractional content of gravel is likely required in order for

664 beach face slope to correspond to bulk median grain size. Grain size distributions of sand serve
665 as the primary governor of beach face permeability and sediment transport in bimodal systems,
666 which together likely explain why it has greater observed control on beach morphology for
667 mixed sand and gravel systems.

668

669 **Acknowledgements**

670 University of Massachusetts undergraduates J. Light, M. Cashman, S. Gessay, S. Osgood, N.
671 Doiron, A. Chica, J. Healey, J. Jurnack, M. Koerth, and P. Southard assisted in the field and lab
672 work. M. Mansfield, R. Haney, J. Burtner, K. Glenn, and J. Knisel from MA Coastal Zone
673 Management gave guidance and logistical support throughout the project. M. Borrelli from
674 UMass-Boston and Center for Coastal Studies and R. Newton of Smith College contributed
675 technical assistance and positioning equipment for beach surveys, and J. Warner assisted with
676 access to COAWST model results. Woodruff is grateful for support by the University of Maine
677 Darling Marine Center which provided residency during the completion of this manuscript. This
678 research was funded by the U.S. Department of Interior, Bureau of Ocean Energy Management
679 under cooperative agreement M14AC00006. The views and conclusions contained in this
680 document are those of the authors and should not be interpreted as representing the opinions or
681 policies of the U.S. Government. Mention of trade names or commercial products does not
682 constitute their endorsement by the U.S. Government.

683

684 **Figure Captions**

685

686 **Figure 1.** Regional Massachusetts coastline (upper left panel) and study area locations shown in
687 panels A-F, along with transect locations (black circles), surficial geology with key provided.
688 Text boxes indicate location of each beach in study as well as its predominant surficial geology
689 (modified from Stone and others, 2018).

690

691 **Figure 2:** (A) Significant wave height - H_{sig} , and (B) combined grain size and (C) beach face
692 slope distributions for summer (orange) and winter (blue) surveys. Beach sites arranged north-to-
693 south (left-to-right). H_{sig} averages (bars) and 12-hr averaged maxima (circles) are over the 30-
694 days prior to surveying. Box plots in B and C include the median (thick horizontal line), bounds
695 average 12-hr maxima and median grain size and slope for meso- and micro- tidal regions shown
696 as dashed horizontal orange and blue lines, respectfully.

697

698 **Figure 3:** Bulk grain size distribution for sites and arranged with respect to their predominant
699 sediment source. Box plots include the median (thick horizontal line), bounds of middle quantiles
700 (boxes) and 10th-to-90th percentiles (thin vertical line).

701

702 **Figure 4:** Composite grain size distribution of binned (blue) and cumulative (red) percent for all
703 intertidal mixed sand and gravel samples (MSG). Here MSG samples are defined as greater than
704 5% of distribution exceeding 2 mm (n=454).

705

706 **Figure 5:** Median (D_{50}) grain size versus beach face slope for low tide (left panel), mid tide
707 (middle panel) and high tide (right panel) compared to the global data set of Bujan et al. (2019).
708 Moderately-to-well sorted samples (circles) and poorly sorted samples (plus markers) are defined

709 by criteria presented by Blott and Pye (2001) . The same global data set from Bujan et al. (2019)
710 is shown in each panel (gray asterisk) where grain sizes represents either a D_{50} or mean and were
711 obtained by a variety of methods provided by references therein.

712

713 **Figure 6:** (A) Median grain size versus beach face slope for MSG (plus signs) and pure sand
714 beaches (black circles) in this study compared to data by Jennings and Schulmeister (2002) for
715 pure gravel beaches (J&S,2002, black triangles). Left panel is bulk D_{50} grain size and right panel
716 is the median grain size of just the isolated sand fraction (i.e. median for distribution < 2 mm).
717 Power law fits (dashed lines) are provided for bulk D_{50} and median size in sand fraction (D_{s50})
718 versus beach face slope (S). Values of best fit for right panel in the form of $S=a*D_{s50}^b+c$ and
719 fitted parameters of $a = -0.10$, $b = -0.37$, and $c = 0.22$.

720

721 **Figure 7:** Beach face slope versus bulk median grain size (left panels) and median grain size for
722 sand fraction (right panels) categorized by tidal region (top panels) and season (bottom panels).

723

724

725 **References**

726

727 Bagnold, R.A., 1940. Beach formation by waves: some model experiments in a wave tank.

728 *Journal of the Institution of Civil Engineers* 15, 27–52.

729 Barnhardt, W.A., Ackerman, S.D., Andrews, B.D., Baldwin, W.E., 2010. Geophysical and

730 sampling data from the inner continental shelf: Duxbury to Hull, Massachusetts. US

731 Geological Survey.

732 Barnhardt, W.A., Andrews, B.D., Ackerman, S.D., Baldwin, W.E., Hein, C.J., 2009. High-

733 Resolution Geologic Mapping of the Inner Continental Shelf: Cape Ann to Salisbury

734 Beach, Massachusetts. US Geological Survey.

735 Bascom, W.N., 1951. The relationship between sand size and beach-face slope. *Eos,*

736 *Transactions American Geophysical Union* 32, 866–874.

737 <https://doi.org/10.1029/TR032i006p00866>

738 Bergillos, R.J., Ortega-Sánchez, M., Masselink, G., Losada, M.A., 2016. Morpho-sedimentary

739 dynamics of a micro-tidal mixed sand and gravel beach, Playa Granada, southern Spain.

740 *Marine Geology* 379, 28–38. <https://doi.org/10.1016/j.margeo.2016.05.003>

741 Billy, J., Robin, N., Hein, C.J., Certain, R., FitzGerald, D.M., 2015. Insight into the late

742 Holocene sea-level changes in the NW Atlantic from a paraglacial beach-ridge plain

743 south of Newfoundland. *Geomorphology* 248, 134–146.

744 <https://doi.org/10.1016/j.geomorph.2015.07.033>

745 Blott, S.J., Pye, K., 2001. GRADISTAT: a grain size distribution and statistics package for the

746 analysis of unconsolidated sediments. *Earth Surface Processes and Landforms* 26, 1237–

747 1248. <https://doi.org/10.1002/esp.261>

- 748 Bluck, B.J., 1967. Sedimentation of beach gravels; examples from South Wales. *Journal of*
749 *Sedimentary Research* 37, 128–156.
- 750 Bujan, N., Cox, R., Masselink, G., 2019. From fine sand to boulders: Examining the relationship
751 between beach-face slope and sediment size. *Marine Geology* 417, 106012.
752 <https://doi.org/10.1016/j.margeo.2019.106012>
- 753 Buscombe, D., Masselink, G., 2006. Concepts in gravel beach dynamics. *Earth-Science Reviews*
754 79, 33–52. <https://doi.org/10.1016/j.earscirev.2006.06.003>
- 755 Caldwell, N.E., Williams, A.T., 1985. The Role of Beach Profile Configuration in the
756 Discrimination between Differing Depositional Environments Affecting Coarse Clastic
757 Beaches. *Journal of Coastal Research* 1, 129–139.
- 758 Carter, R.W.G., Forbes, D.L., Jennings, S.C., Orford, J.D., Shaw, J., Taylor, R.B., 1989. Barrier
759 and lagoon coast evolution under differing relative sea-level regimes: examples from
760 Ireland and Nova Scotia. *Marine Geology* 88, 221–242. [https://doi.org/10.1016/0025-](https://doi.org/10.1016/0025-3227(89)90099-6)
761 [3227\(89\)90099-6](https://doi.org/10.1016/0025-3227(89)90099-6)
- 762 Carter, R.W.G., Johnston, T.W., McKenna, J., Orford, J.D., 1987. Sea-level, sediment supply
763 and coastal changes: examples from the coast of Ireland. *Progress in Oceanography* 18,
764 79–101.
- 765 Carter, R.W.G., Orford, J.D., 1993. The Morphodynamics of Coarse Clastic Beaches and
766 Barriers: A Short- and Long-term Perspective. *Journal of Coastal Research* 158–179.
- 767 Carter, R.W.G., Orford, J.D., 1984. Coarse clastic barrier beaches: a discussion of the distinctive
768 dynamic and morphosedimentary characteristics, in: *Developments in Sedimentology*.
769 Elsevier, pp. 377–389.

- 770 Dade, W.B., Friend, P.F., 1998. Grain-Size, Sediment-Transport Regime, and Channel Slope in
771 Alluvial Rivers. *The Journal of Geology* 106, 661–676. <https://doi.org/10.1086/516052>
- 772 Dingle, E.H., Sinclair, H.D., Venditti, J.G., Attal, M., Kinnaird, T.C., Creed, M., Quick, L.,
773 Nittrouer, J.A., Gautam, D., 2020. Sediment dynamics across gravel-sand transitions:
774 Implications for river stability and floodplain recycling. *Geology* 48, 468–472.
775 <https://doi.org/10.1130/G46909.1>
- 776 DiPietro, J.A., 2012. Landscape evolution in the United States: an introduction to the geography,
777 geology, and natural history. Elsevier.
- 778 DiTroia, A., 2019. Legacy Sediment Controls on Post-Glacial Beaches of Massachusetts
779 (Masters Theses). University of Massachusetts, Amherst, MA USA.
- 780 Dreimanis, A., Vagners, U.J., 1971. Bimodal distribution of rock and mineral fragments in basal
781 tills, in: Goldthwait, R.P. (Ed.), *Till, a Symposium*. Ohio State University Press,
782 Columbus, Ohio, pp. 237–250.
- 783 Dubois, R.N., 1972. Inverse relation between foreshore slope and mean grain size as a function
784 of the heavy mineral content. *Geological Society of America Bulletin* 83, 871–876.
- 785 Dunne, K.B.J., Jerolmack, D.J., 2018. Evidence of, and a proposed explanation for, bimodal
786 transport states in alluvial rivers. *Earth Surf. Dynam.* 6, 583–594.
787 <https://doi.org/10.5194/esurf-6-583-2018>
- 788 Easterbrook, D.J., 1982. Characteristic features of glacial sediments, in: *Sandstone Depositional*
789 *Environments*. American Association of Petroleum Geologists.
- 790 Emery, K.O., 1955. Grain Size of Marine Beach Gravels. *The Journal of Geology* 63, 39–49.

- 791 Emery, K.O., Wigley, R.L., Bartlett, A.S., Rubin, M., Barghoorn, E.S., 1967. Freshwater peat on
792 the continental shelf. *Science* 158, 1301–1307.
793 <https://doi.org/10.1126/science.158.3806.1301>
- 794 Engelhart, S.E., Horton, B.P., 2012. Holocene sea level database for the Atlantic coast of the
795 United States. *Quaternary Science Reviews* 54, 12–25.
- 796 Eynon, G., Walker, R.G., 1974. Facies relationships in Pleistocene outwash gravels, southern
797 Ontario: a model for bar growth in braided rivers. *Sedimentology* 21, 43–70.
- 798 Fenneman, N.M., 1938. *Physiography of Eastern United States*.
- 799 Fenneman, N.M., 1917. Physiographic divisions of the United States. *Proc. Natl. Acad. Sci.* 3,
800 17–22.
- 801 Fenneman, N.M., 1916. Physiographic divisions of the United States. *Ann. Assoc. Amer. Geog.*
802 6, 19–98.
- 803 Ferguson, R., Hoey, T., Wathen, S., Werritty, A., 1996. Field evidence for rapid downstream
804 fining of river gravels through selective transport. *Geology* 24, 179–182.
- 805 Ferguson, R.I., 2003. Emergence of abrupt gravel to sand transitions along rivers through sorting
806 processes. *Geology* 31, 159–162.
- 807 Finch, J., 1823. *Geological Essay on the Tertiary Formations in America...*
- 808 FitzGerald, D.M., Rosen, P.S., 1988. USA--Massachusetts, in: Walker, H.J. (Ed.), *Artificial*
809 *Structures and Shorelines*, The GeoJournal Library. Springer, pp. 545–560.
- 810 Fitzgerald, D.M., Van Heteren, S., 1999. Classification of paraglacial barrier systems: coastal
811 New England, USA. *Sedimentology* 46, 1083–1108. [https://doi.org/10.1046/j.1365-](https://doi.org/10.1046/j.1365-3091.1999.00266.x)
812 [3091.1999.00266.x](https://doi.org/10.1046/j.1365-3091.1999.00266.x)

- 813 Folk, R.L., Ward, W.C., 1957. Brazos River Bar: A Study in the Significance of Grain Size
814 Parameters. *Journal of Sedimentary Petrology* 27, 3–26.
- 815 Forbes, D.L., Orford, J.D., Carter, R.W.G., Shaw, J., Jennings, S.C., 1995. Morphodynamic
816 evolution, self-organisation, and instability of coarse-clastic barriers on paraglacial
817 coasts. *Marine Geology* 126, 63–85. [https://doi.org/10.1016/0025-3227\(95\)00066-8](https://doi.org/10.1016/0025-3227(95)00066-8)
- 818 Forbes, D.L., Syvitski, J.P., 1994. Paraglacial coasts. *Coastal Evolution: Late Quaternary*
819 *Shoreline Morphodynamics*. Cambridge University Press, Cambridge 373–424.
- 820 Haldorsen, S., 2008. Grain-size distribution of subglacial till and its relation to glacial crushing
821 and abrasion. *Boreas* 10, 91–105. <https://doi.org/10.1111/j.1502-3885.1981.tb00472.x>
- 822 Hayes, M.O., 1979. Barrier island morphology as a function of tidal and wave regime. In:
823 Leatherman SP (ed) *Barrier Islands*. Academic Press, New York 1, 27.
- 824 Hayes, M.O., Ruby, C.H., 1994. Barriers of Pacific Alaska, in: *Geology of Holocene Barrier*
825 *Island Systems*. Springer, Berlin, Heidelberg, pp. 395–433.
- 826 Hein, C.J., Fallon, A.R., Rosen, P., Hoagland, P., Georgiou, I.Y., FitzGerald, D.M., Morris, M.,
827 Baker, S., Marino, G.B., Fitzsimons, G., 2019. Shoreline Dynamics Along a Developed
828 River Mouth Barrier Island: Multi-Decadal Cycles of Erosion and Event-Driven
829 Mitigation. *Front. Earth Sci.* 7, 103. <https://doi.org/10.3389/feart.2019.00103>
- 830 Hein, C.J., FitzGerald, D.M., Buynevich, I.V., Van Heteren, S., Kelley, J.T., 2014. Evolution of
831 paraglacial coasts in response to changes in fluvial sediment supply. *Geological Society*,
832 London, Special Publications 388, 247–280.
- 833 Holmes, P., Baldock, T.E., Chan, R.T., Neshaei, M.A.L., 1996. Beach evolution under random
834 waves. Presented at the 25th International Conference on Coastal Engineering, pp. 3006–
835 3019.

- 836 Horn, D.P., 2002. Beach groundwater dynamics. *Geomorphology* 48, 121–146.
837 [https://doi.org/10.1016/S0169-555X\(02\)00178-2](https://doi.org/10.1016/S0169-555X(02)00178-2)
- 838 Horn, D.P., Walton, S.M., 2007. Spatial and temporal variations of sediment size on a mixed
839 sand and gravel beach. *Sedimentary Geology* 202, 509–528.
840 <https://doi.org/10.1016/j.sedgeo.2007.03.023>
- 841 Hsieh, M.-L., Liew, P.-M., Hsu, M.-Y., 2004. Holocene tectonic uplift on the Hua-tung coast,
842 eastern Taiwan. *Quaternary International* 115–116, 47–70.
843 [https://doi.org/10.1016/S1040-6182\(03\)00096-X](https://doi.org/10.1016/S1040-6182(03)00096-X)
- 844 Inman, D.L., 1949. Sorting of sediments in the light of fluid mechanics. *Journal of Sedimentary*
845 *Research* 19, 51–70.
- 846 Irish, J.D., Signell, R.P., 1992. *Tides of Massachusetts and Cape Cod Bays*. Woods Hole
847 Oceanographic Institution.
- 848 Ivamy, M.C., Kench, P.S., 2006. Hydrodynamics and morphological adjustment of a mixed sand
849 and gravel beach, Torere, Bay of Plenty, New Zealand. *Marine Geology* 228, 137–152.
850 <https://doi.org/10.1016/j.margeo.2006.01.002>
- 851 Jennings, R., Shulmeister, J., 2002. A field based classification scheme for gravel beaches.
852 *Marine Geology* 186, 211–228.
- 853 Jennings, S., Smyth, C., 1990. Holocene evolution of the gravel coastline of East Sussex.
854 *Proceedings of the Geologists' Association* 101, 213–224.
- 855 Jerolmack, D.J., Brzinski, T.A., 2010. Equivalence of abrupt grain-size transitions in alluvial
856 rivers and eolian sand seas: A hypothesis. *Geology* 38, 719–722.
857 <https://doi.org/10.1130/G30922.1>

- 858 Kelley, J.T., 1987. An Inventory of Coastal Environments and Classification of Maine's
859 Glaciated Shoreline, in: FitzGerald, D.M., Rosen, P.S. (Eds.), *Glaciated Coasts*.
860 Academic Press, Inc, San Diego, pp. 151–176.
- 861 Kirk, R.M., 1980. Mixed sand and gravel beaches: morphology, processes and sediments.
862 *Progress in Physical Geography* 4, 189–210.
- 863 Koteff, C., Pessl, F., 1981. Systematic ice retreat in New England (U.S. Geological Survey
864 Professional Paper No. 1179).
- 865 Krumbein, W.C., Monk, G.D., 1943. Permeability as a function of the size parameters of
866 unconsolidated sand. *Transactions of the AIME* 151, 153–163.
- 867 Lamb, M.P., Venditti, J.G., 2016. The grain size gap and abrupt gravel-sand transitions in rivers
868 due to suspension fallout. *Geophysical Research Letters* 43, 3777–3785.
869 <https://doi.org/10.1002/2016GL068713>
- 870 Luijendijk, A., Hagenaars, G., Ranasinghe, R., Baart, F., Donchyts, G., Aarninkhof, S., 2018.
871 The State of the World's Beaches. *Sci Rep* 8, 6641. [https://doi.org/10.1038/s41598-018-](https://doi.org/10.1038/s41598-018-24630-6)
872 [24630-6](https://doi.org/10.1038/s41598-018-24630-6)
- 873 Maizels, J., 1993. Lithofacies variations within sandur deposits: the role of runoff regime, flow
874 dynamics and sediment supply characteristics. *Sedimentary Geology* 85, 299–325.
875 [https://doi.org/10.1016/0037-0738\(93\)90090-R](https://doi.org/10.1016/0037-0738(93)90090-R)
- 876 Marr, J.G., Swenson, J.B., Paola, C., Voller, V.R., 2000. A two-diffusion model of fluvial
877 stratigraphy in closed depositional basins. *Basin Research* 12, 381–398.
878 <https://doi.org/10.1111/j.1365-2117.2000.00134.x>

- 879 Martínez, M.L., Intralawan, A., Vázquez, G., Pérez-Maqueo, O., Sutton, P., Landgrave, R., 2007.
880 The coasts of our world: Ecological, economic and social importance. *Ecological*
881 *Economics* 63, 254–272. <https://doi.org/10.1016/j.ecolecon.2006.10.022>
- 882 Mason, T., Coates, T.T., 2001. Sediment Transport Processes on Mixed Beaches: A Review for
883 Shoreline Management. *Journal of Coastal Research* 17, 645–657.
- 884 Mason, T., Voulgaris, G., Simmonds, D.J., Collins, M.B., 1997. Hydrodynamics and sediment
885 transport on composite (mixed sand/shingle) and sand beaches: A comparison, in:
886 Thornton, E.B. (Ed.), *Coastal Dynamics*. American Society of Civil Engineers, New
887 York, pp. 48–57.
- 888 Masselink, G., Hughes, M., 1998. Field investigation of sediment transport in the swash zone.
889 *Continental Shelf Research* 18, 1179–1199. [https://doi.org/10.1016/S0278-](https://doi.org/10.1016/S0278-4343(98)00027-2)
890 [4343\(98\)00027-2](https://doi.org/10.1016/S0278-4343(98)00027-2)
- 891 Masselink, G., Li, L., 2001. The role of swash infiltration in determining the beachface gradient:
892 a numerical study. *Marine Geology* 176, 139–156.
- 893 Masselink, G., Russell, P., Blenkinsopp, C., Turner, I., 2010. Swash zone sediment transport,
894 step dynamics and morphological response on a gravel beach. *Marine Geology* 274, 50–
895 68. <https://doi.org/10.1016/j.margeo.2010.03.005>
- 896 Masselink, G., Short, A.D., 1993. The Effect of Tide Range on Beach Morphodynamics and
897 Morphology: A Conceptual Beach Model. *Journal of Coastal Research* 9, 785–800.
- 898 Masterson, J.P., Stone, B.D., Walter, D.A., Savoie, J.G., 1997. Hydrogeologic framework of
899 western Cape Cod, Massachusetts (U.S. Geological Survey Hydrologic Investigations
900 Atlas No. 741).

- 901 Mather, K.F., Goldthwait, R.P., Thiesmeyer, L.R., 1942. Pleistocene geology of western Cape
902 Cod, Massachusetts. *Bulletin of the Geological Society of America* 53, 1127–1174.
- 903 McLean, R.F., 1970. Variations in grain-size and sorting on two kaikoura beaches. *New Zealand*
904 *Journal of Marine and Freshwater Research* 4, 141–164.
905 <https://doi.org/10.1080/00288330.1970.9515334>
- 906 McLean, R.F., Kirk, R.M., 1969. Relationships between grain size, size-sorting, and foreshore
907 slope on mixed sand - shingle beaches. *New Zealand Journal of Geology and Geophysics*
908 12, 138–155. <https://doi.org/10.1080/00288306.1969.10420231>
- 909 Ockay, C., Hubert, J.F., 1996. Mineralogy and provenance of Pleistocene outwash-plain and
910 modern beach sands of outer Cape Cod, Massachusetts, USA. *Marine Geology* 130, 121–
911 137. [https://doi.org/10.1016/0025-3227\(95\)00125-5](https://doi.org/10.1016/0025-3227(95)00125-5)
- 912 Oldale, R.N., Barlow, R.A., 1986. Geologic map of Cape Cod and the islands, Massachusetts
913 (Miscellaneous Investigations Series Map No. I-1763). United States Geological Survey.
- 914 Oldale, R.N., Colman, S.M., Jones, G.A., 1993. Radiocarbon ages from two submerged
915 strandline features in the western Gulf of Maine and a sea-level curve for the northeastern
916 Massachusetts coastal region. *Quaternary Research* 40, 38–45.
- 917 Orford, J.D., Forbes, D.L., Jennings, S.C., 2002. Organisational controls, typologies and time
918 scales of paraglacial gravel-dominated coastal systems. *Geomorphology* 48, 51–85.
919 [https://doi.org/10.1016/S0169-555X\(02\)00175-7](https://doi.org/10.1016/S0169-555X(02)00175-7)
- 920 Orford, J.D., Jennings, S.C., Forbes, D.L., 2001. Origin, development, reworking and breakdown
921 of gravel-dominated coastal barriers in Atlantic Canada: future scenarios for the British
922 coast, in: Packham, J.R., Barnes, R.S.K., Neals, A. (Eds.), *Ecology & Geomorphology of*
923 *Coastal Shingle*. Westbury, pp. 23–55.

- 924 Ortega-Sánchez, M., Bergillos, R.J., López-Ruiz, A., Losada, M.A., 2017. Morphodynamics of
925 mediterranean mixed sand and gravel coasts. Springer.
- 926 Paola, C., Heller, P.L., Angevine, C.L., 1992. The large-scale dynamics of grain-size variation in
927 alluvial basins, 1: Theory. *Basin research* 4, 73–90.
- 928 Parker, G., Cui, Y., 1998. The arrested gravel front: stable gravel-sand transitions in rivers Part
929 1: Simplified analytical solution. *Journal of hydraulic research* 36, 75–100.
- 930 Peltier, W.R., 2004. Global glacial isostasy and the surface of the ice-age Earth: the ICE-5G
931 (VM2) model and GRACE. *Annu. Rev. Earth Planet. Sci.* 32, 111–149.
- 932 Pontee, N.I., Pye, K., Blott, S.J., 2004. Morphodynamic Behaviour and Sedimentary Variation of
933 Mixed Sand and Gravel Beaches, Suffolk, UK. *Journal of Coastal Research* 20, 256–276.
- 934 Pratt, R.M., Schlee, J., 1969. Glaciation on the Continental Margin off New England. *Geol Soc
935 America Bull* 80, 2335–2342. [https://doi.org/10.1130/0016-
936 7606\(1969\)80\[2335:GOTCMO\]2.0.CO;2](https://doi.org/10.1130/0016-7606(1969)80[2335:GOTCMO]2.0.CO;2)
- 937 Quick, M.C., Dyksterhuis, P., 1994. Cross-shore transport for beaches of mixed sand and gravel,
938 in: *International Symposium: Waves—Physical and Numerical Modeling*. Canadian
939 Society of Civil Engineers. pp. 1443–1452.
- 940 Rădoane, M., Rădoane, N., Dumitriu, D., Miclăuș, C., 2008. Downstream variation in bed
941 sediment size along the East Carpathian rivers: evidence of the role of sediment sources.
942 *Earth Surface Processes and Landforms* 33, 674–694. <https://doi.org/10.1002/esp.1568>
- 943 Redfield, A.C., 1980. *The tides of the waters of New England and New York*. Woods Hole
944 Oceanographic Institution.

- 945 Robinson, R.A.J., Slingerland, R.L., 1998. Origin of fluvial grain-size trends in a foreland basin;
946 the Pocono Formation on the central Appalachian Basin. *Journal of Sedimentary*
947 *Research* 68, 473–486. <https://doi.org/10.2110/jsr.68.473>
- 948 Sambrook-Smith, G.H., 1996. Bimodal fluvial bed sediments: origin, spatial extent and
949 processes. *Progress in Physical Geography* 20, 402–417.
- 950 Sambrook-Smith, G.H., Ferguson, R.I., 1995. The Gravel-Sand Transition Along River Channels.
951 *SEPM JSR A65*, 423–430. [https://doi.org/10.1306/D42680E0-2B26-11D7-](https://doi.org/10.1306/D42680E0-2B26-11D7-8648000102C1865D)
952 [8648000102C1865D](https://doi.org/10.1306/D42680E0-2B26-11D7-8648000102C1865D)
- 953 Sambrook-Smith, G.H., Nicholas, A.P., Ferguson, R.I., 1997. Measuring and defining bimodal
954 sediments: Problems and implications. *Water Resources Research* 33, 1179–1185.
955 <https://doi.org/10.1029/97WR00365>
- 956 Shaw, J., Kellerhals, R., 1982. The composition of recent alluvial gravels in Alberta river beds,
957 *Bull.* 41, 151 pp. *Alberta Research Council Bulletin* 41, 151.
- 958 Shulmeister, J., Kirk, R.M., 1997. Holocene fluvial-coastal interactions on a mixed sand and
959 sand and gravel beach system, North Canterbury, New Zealand. *Catena* 30, 337–355.
- 960 Stone, B.D., DiGiacomo-Cohen, M.L., 2006. Surficial geologic map of the Pocasset-
961 Provincetown-Cuttyhunk-Nantucket 24-quadrangle area of Cape Cod and Islands,
962 southeast Massachusetts (Open-File Report No. 2006-1260- E). United States Geological
963 Survey.
- 964 Stone, B.D., Stone, J.R., 2019. Geologic origins of Cape Cod, Massachusetts; Guidebook for the
965 Northeast Friends of the Pleistocene (Massachusetts Geological Survey Open-file Report
966 No. 19– 01).

- 967 Stone, B.D., Stone, J.R., DiGiacomo-Cohen, M.L., 2006. Surficial geologic map of the Salem
968 Depot-Newburyport East-Wilmington-Rockport 16-quadrangle area in northeast
969 Massachusetts (Open File Report No. 2006-1260- B). United States Geological Survey.
- 970 Stone, B.D., Stone, J.R., DiGiacomo-Cohen, M.L., Kincare, K.A., 2012. Surficial geologic map
971 of the Norton-Manomet-Westport-Scotcut Neck 23-quadrangle area in southeast
972 Massachusetts (No. Open-File Report 2006–1260–F). United States Geological Survey.
- 973 Stone, B.D., Stone, J.R., Masterson, J.P., O’Leary, D.W., 2004a. Integrating 3-D facies analysis
974 of glacial aquifer systems with ground-water flow models: Examples from New England
975 and the Great Lakes Region, USA (Open-file Series No. 2004–8). Illinois State
976 Geological Survey.
- 977 Stone, B.D., Stone, J.R., McWeeney, L.J., 2004b. Where the glacier met the sea: Late
978 Quaternary geology of the northeast coast of Massachusetts from Cape Ann to Salisbury,
979 in: Proceedings of the New England Intercollegiate Geological Conference, Salem,
980 Massachusetts, B-3. p. 25.
- 981 Stone, J.R., Stone, B.D., DiGiacomo-Dohen, M., L., Mabee, S.B., 2018. Surficial materials of
982 Massachusetts—A 1:24,000-scale geologic map database. Scientific Investigations Map
983 3402. <https://doi.org/10.3133/sim3402>
- 984 Switzer, A.D., Pile, J., 2015. Grain size analysis, in: Shennan, I., Long, A.J., Horton, B.P. (Eds.),
985 Handbook of Sea-Level Research. John Wiley & Sons, Ltd., pp. 331–346.
- 986 Udden, J.A., 1914. Mechanical composition of clastic sediments. Bulletin of the Geological
987 Society of America 25, 655–744. <https://doi.org/doi:10.1130/GSAB-25-655>
- 988 U.S. National Park Service, 2017. Physiographic Provinces - Geology [WWW Document]. URL
989 <https://www.nps.gov/subjects/geology/physiographic-provinces.htm> (accessed 8.25.20).

- 990 USACE, (U.S. Army Corps of Engineers), 2012. Nantasket Beach, Hull, MA Seawall Impacts on
991 Beach Erosion [WWW Document]. URL
992 [https://www.yumpu.com/en/document/view/49940207/nantasket-beach-hull-ma-seawall-](https://www.yumpu.com/en/document/view/49940207/nantasket-beach-hull-ma-seawall-impacts-on-beach-fsbpa)
993 [impacts-on-beach-fsbpa](https://www.yumpu.com/en/document/view/49940207/nantasket-beach-hull-ma-seawall-impacts-on-beach-fsbpa) (accessed 8.26.20).
- 994 Wentworth, C.K., 1922. A scale of grade and class terms for clastic sediments. *The Journal of*
995 *Geology* 30, 377–392.
- 996 Wolcott, J., 1988. Nonfluvial Control of Bimodal Grain-Size Distributions in River-Bed Gravels.
997 *SEPM JSR* 58, 979–984. [https://doi.org/10.1306/212F8ED6-2B24-11D7-](https://doi.org/10.1306/212F8ED6-2B24-11D7-8648000102C1865D)
998 [8648000102C1865D](https://doi.org/10.1306/212F8ED6-2B24-11D7-8648000102C1865D)
- 999 Wolman, M.G., 1954. A method of sampling coarse river-bed material. *Eos, Transactions*
1000 *American Geophysical Union* 35, 951–956. <https://doi.org/10.1029/TR035i006p00951>
- 1001 Woolf, D.K., Challenor, P.G., Cotton, P.D., 2002. Variability and predictability of the North
1002 Atlantic wave climate. *Journal of Geophysical Research: Oceans* 107, 9-1-9–14.
1003 <https://doi.org/10.1029/2001JC001124>
- 1004 Zenkovich, V.P., 1967. *Processes of coastal development*. Oliver and Boyd, London.
- 1005 Zervas, C.E., 2009. *Sea level variations of the United States, 1854-2006* (Technical Report No.
1006 NOS CO-OPS 053). NOAA.
- 1007

Table 1. General characteristics of beaches, Massachusetts, USA

Beach ¹	Tide Range (m)	Average Wave Height (m) ²	Wave Height Standard Dev. (m)	Geomorphic Setting ³	Dominant Source Material ⁴
Salisbury	2.7	0.9	0.3	Inlet-Segmented	Coarse Stratified Deposits
Plum Island	2.7	0.9	0.3	Inlet-Segmented	Coarse Stratified Deposits
Rockport	2.7	1.8	1.0	Headland-Separated	Till
Nahant	2.8	0.8	0.2	Headland-Separated	Fine Stratified Deposits
Revere	2.8	0.8	0.2	Headland-Separated	Fine Stratified Deposits
Nantasket	2.8	0.8	0.2	Headland-Separated	Till
Peggotty	2.7	0.9	0.6	Headland-Separated	Mixed
Humarock	2.8	0.9	0.6	Headland-Separated	Mixed
Marshfield	2.8	0.8	0.6	Headland-Separated	Mixed
Plymouth	2.9	0.7	0.6	Mainland-Segmented	Coarse Stratified Deposits
Surf	0.6	0.7	0.4	Mainland-Segmented	Mixed
Low	0.9	1.8	0.9	Mainland-Segmented	Coarse Stratified Deposits
Miacomet	0.9	1.7	0.8	Mainland-Segmented	Coarse Stratified Deposits
Town	0.6	0.6	0.3	Mainland-Segmented	Mixed
Sylvia	0.6	0.6	0.3	Mainland-Segmented	Mixed
Barges	1.0	1.2	0.6	Headland-Separated	Till
East	1.1	1.2	0.6	Headland-Separated	Till
Horseneck	1.1	1.2	0.6	Headland-Separated	Till

¹ Study sites at Rockport, Nahant, and Plymouth are referred to colloquially as “Long Beach.” The study site at Marshfield aggregates the coast between Rexhame Beach and Brant Rock and includes Fieldston Beach. We instead refer to these by their respective municipalities.

² Average significant wave heights along with standard deviations for the 18 sites over model simulations for years 2014 through 2016 where simulations are available every hour over this interval; data taken from nearest deep-water grid cell (i.e. depth > Lo/2) (Warner and others, 2010).

³ From FitzGerald and van Heteran, (1999).

⁴ Coarse stratified deposits = glacial outwash, delta deposits; fine stratified deposits = fine-grained glacial marine sediments; till = derived from ground moraine or erosion of drumlins; mixed = combination of two source materials, glacial till and coarse stratified deposits in various proportions.

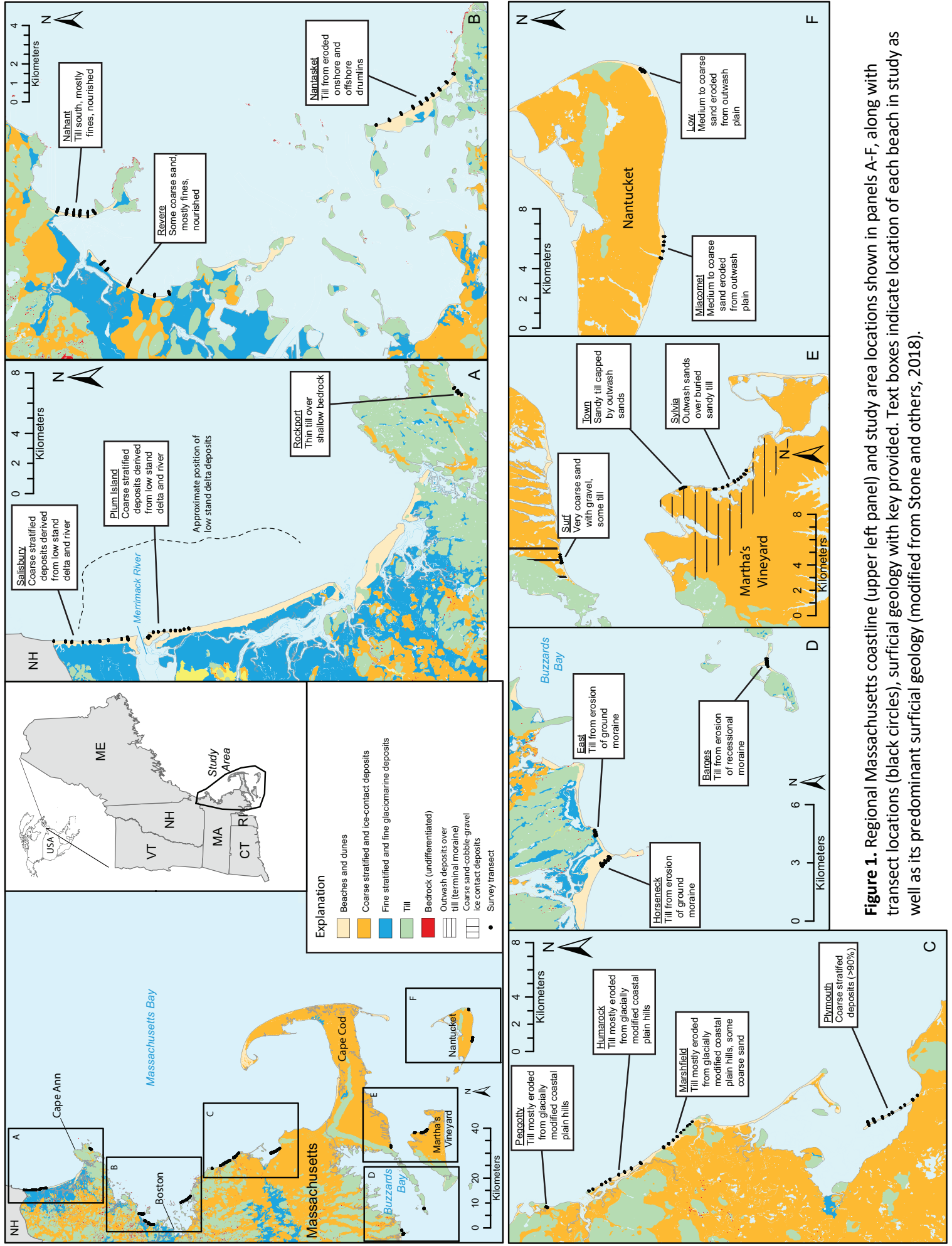


Figure 1. Regional Massachusetts coastline (upper left panel) and study area locations shown in panels A-F, along with transect locations (black circles), surficial geology with key provided. Text boxes indicate location of each beach in study as well as its predominant surficial geology (modified from Stone and others, 2018).

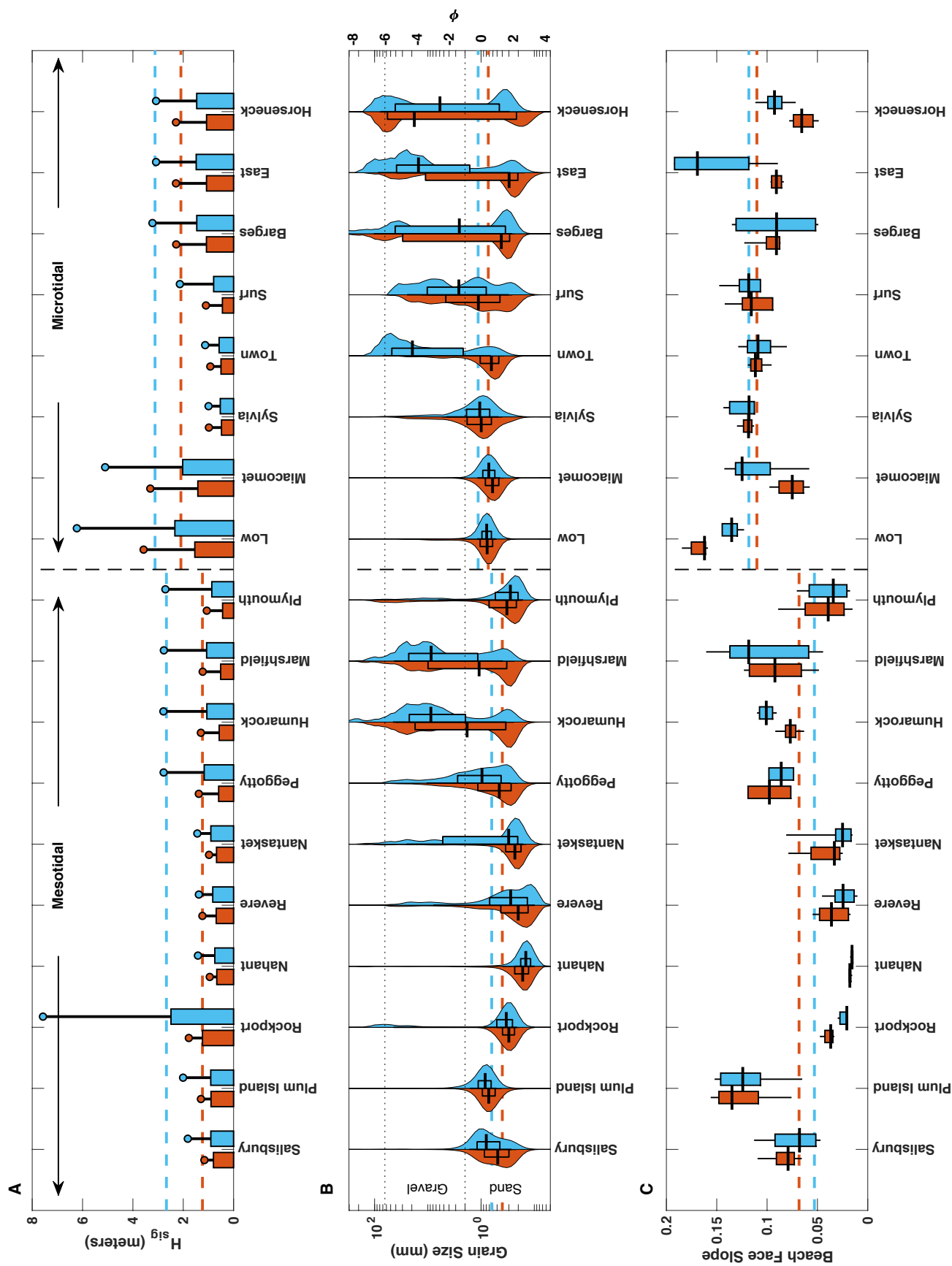


Figure 2: (A) Significant wave height - H_{sig} , and (B) combined grain size and (C) beach face slope distributions for summer (orange) and winter (blue) surveys. Beach sites arranged north-to-south (left-to-right). H_{sig} averages (bars) and 12-hr averaged maxima (circles) are over the 30-days prior to surveying. Box plots in B and C include the median (thick horizontal line), bounds of middle quantiles (boxes) and 10th-to-90th percentiles (thin vertical line). Summer and winter average 12-hr maxima and median grain size and slope for meso- and micro- tidal regions shown as dashed horizontal orange and blue lines, respectively.

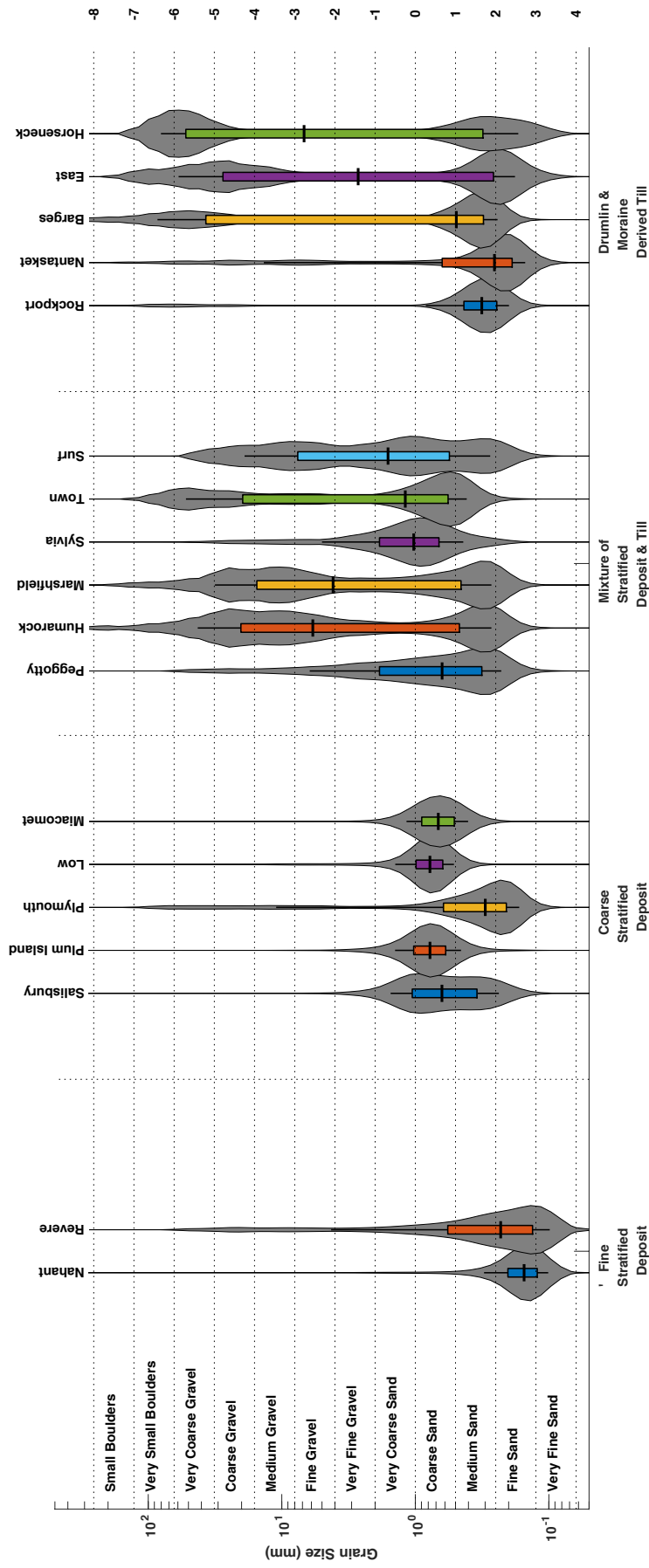


Figure 3: Bulk grain size distribution for sites and arranged with respect to their predominant sediment source. Box plots include the median (thick horizontal line), bounds of middle quantiles (boxes) and 10th-to-90th percentiles (thin vertical line).

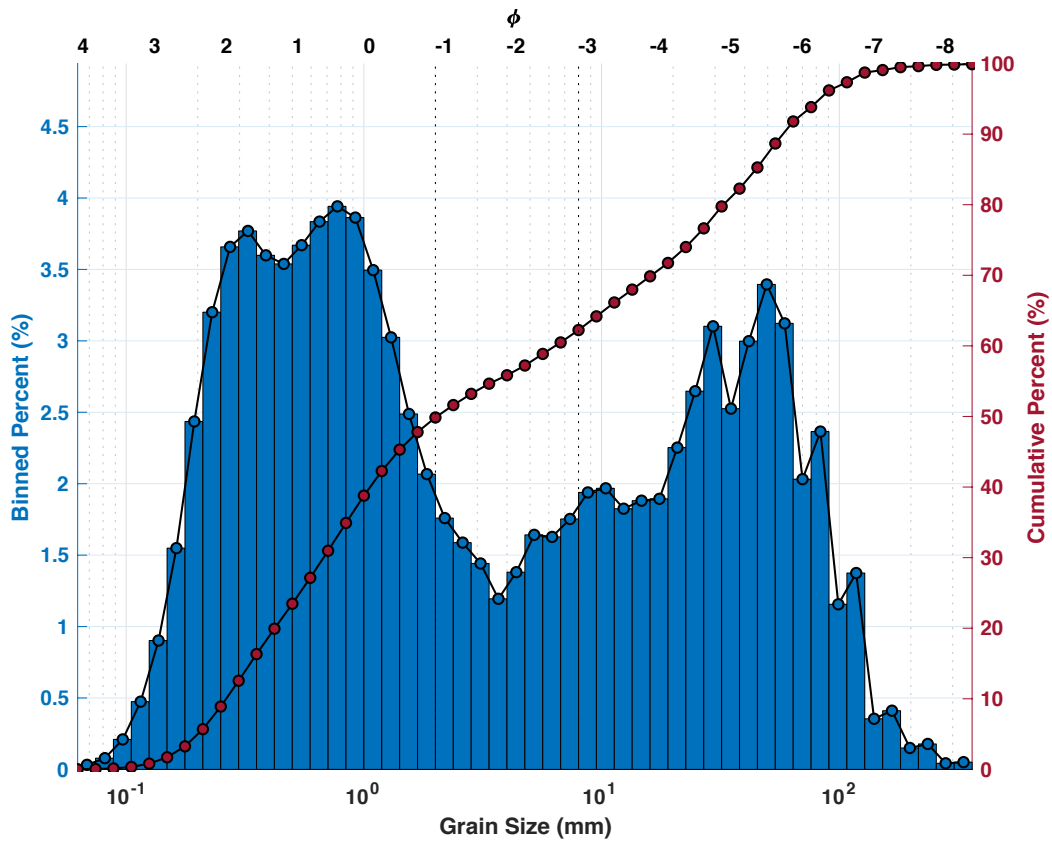


Figure 4: Composite grain size distribution of binned (blue) and cumulative (red) percent for all intertidal mixed sand and gravel samples (MSG). Here MSG samples are defined as greater than 5% of distribution exceeding 2 mm (n=454).

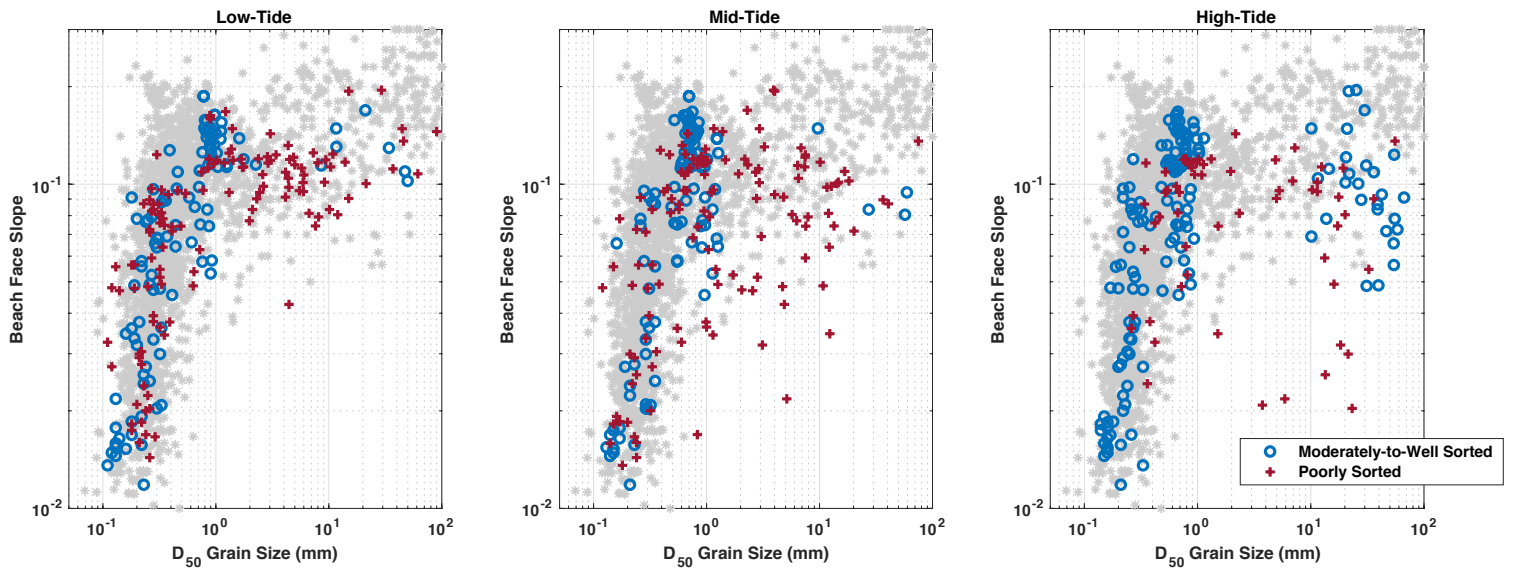


Figure 5: Median (D_{50}) grain size versus beach face slope for low tide (left panel), mid tide (middle panel) and high tide (right panel) compared to the global data set of Bujan et al. (2019). Moderately-to-well sorted samples (circles) and poorly sorted samples (plus markers) are defined by criteria presented by Blott and Pye (2001). The same global data set from Bujan et al. (2019) is shown in each panel (gray asterisk) where grain sizes represents either a D_{50} or mean and were obtained by a variety of methods provided by references therein.

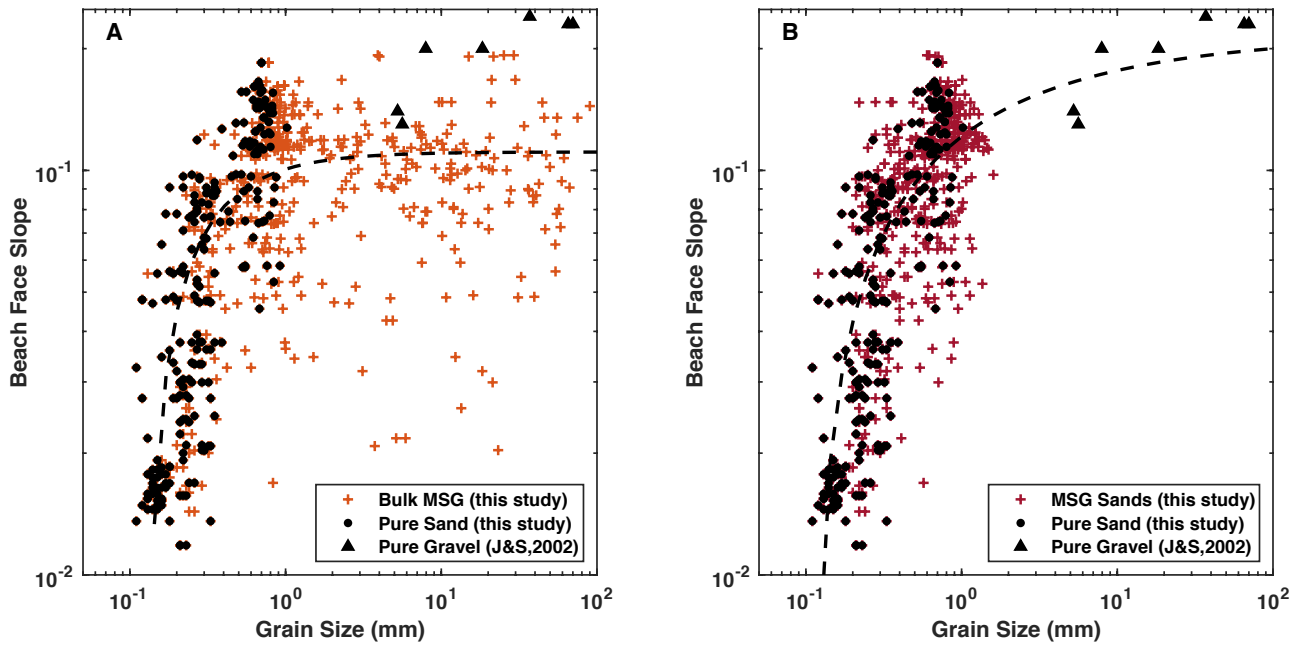


Figure 6: (A) Median grain size versus beach face slope for MSG (plus signs) and pure sand beaches (black circles) in this study compared to data by Jennings and Schulmeister (2002) for pure gravel beaches (J&S,2002, black triangles). Left panel is bulk D_{50} grain size and right panel is the median grain size of just the isolated sand fraction (i.e. median for distribution < 2 mm). Power law fits (dashed lines) are provided for bulk D_{50} and median size in sand fraction (D_{s50}) versus beach face slope (S). Values of best fit for right panel in the form of $S = a * D_{s50}^b + c$ and fitted parameters of $a = -0.10$, $b = -0.37$, and $c = 0.22$.

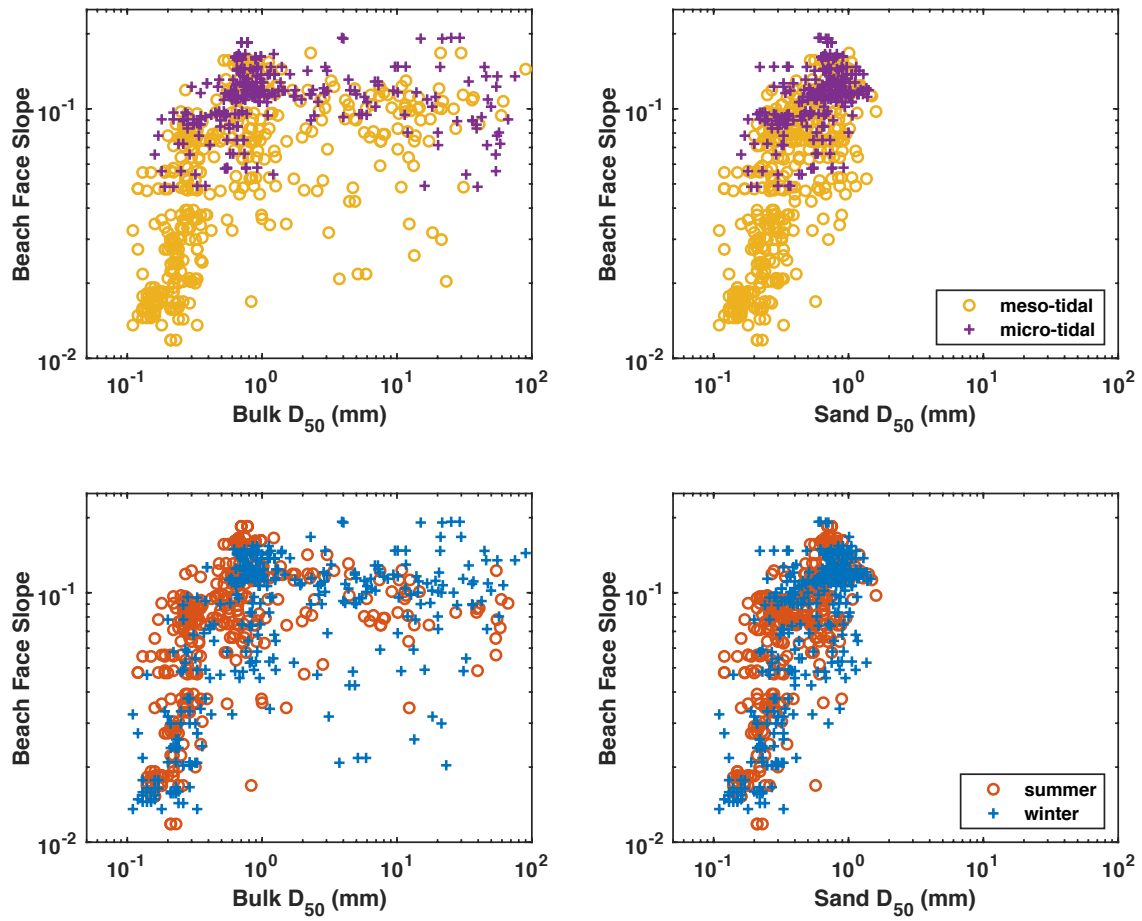


Figure 7: Beach face slope versus bulk median grain size (left panels) and median grain size for sand fraction (right panels) categorized by tidal region (top panels) and season (bottom panels).